1993

Spectral analysis of synoptic time scale disturbances over the tropical eastern Pacific during summer 1989, 1990 and 1991

Swett, William Christopher

Monterey, California. Naval Postgraduate School

http://hdl.handle.net/10945/39900

NAVAL POSTGRADUATE SCHOOL

Monterey, California

THESIS

SPECTRAL ANALYSIS OF SYNOPTIC TIME SCALE DISTURBANCES OVER THE TROPICAL EASTERN PACIFIC DURING SUMMER 1989, 1990 AND 1991

by

William Christopher Swett

March 1993

Thesis Advisor:	Chih-Pei Chang
Co-Advisor:	Tom Murphree

UNCLASSIFIED

SECURITY CLASSIFICATION OF THIS PAGE

REPORT DOCUMENTATION PAGE

1a. REPORT SECURITY CLASSIFICATION
UNCLASSIFIED

1b. RESTRICTIVE MARKINGS

2a. SECURITY CLASSIFICATION AUTHORITY

2b. DECLASSIFICATION/DOWNGRADING SCHEDULE

3. DISTRIBUTION/AVAILABILITY OF REPORT
Approved for public release; distribution is unlimited.

4. PERFORMING ORGANIZATION REPORT NUMBER(S)

5. MONITORING ORGANIZATION REPORT NUMBER(S)

6a. NAME OF PERFORMING ORGANIZATION
Naval Postgraduate School

6b. OFFICE SYMBOL *(If applicable)*
35

7a. NAME OF MONITORING ORGANIZATION
Naval Postgraduate School

6c. ADDRESS *(City, State, and ZIP Code)*
Monterey, CA 93943-5000

7b. ADDRESS *(City, State, and ZIP Code)*
Monterey, CA 93943-5000

8a. NAME OF FUNDING/SPONSORING ORGANIZATION

8b. OFFICE SYMBOL *(If applicable)*

9. PROCUREMENT INSTRUMENT IDENTIFICATION NUMBER

8c. ADDRESS *(City, State, and ZIP Code)*

10. SOURCE OF FUNDING NUMBERS

Program Element No	Project No	Task No	Work Unit Accession Number

11. TITLE *(Include Security Classification)*
SPECTRAL ANALYSIS OF SYNOPTIC TIME SCALE DISTURBANCES OVER THE TROPICAL EASTERN PACIFIC DURING SUMMER 1989, 1990 AND 1991 (U)

12. PERSONAL AUTHOR(S) Swett, William C.

13a. TYPE OF REPORT	13b. TIME COVERED	14. DATE OF REPORT *(year, month, day)*	15. PAGE COUNT
Master's Thesis	From To	*1993 March 25*	93

16. SUPPLEMENTARY NOTATION
The views expressed in this thesis are those of the author and do not reflect the official policy or position of the Department of Defense or the U.S. Government.

17. COSATI CODES

FIELD	GROUP	SUBGROUP

18. SUBJECT TERMS *(continue on reverse if necessary and identify by block number)*
SPECTRAL ANALYSIS, TROPOSPHERIC WAVES, NOGAPS

19. ABSTRACT *(continue on reverse if necessary and identify by block number)*

In this study we used data analyzed by the Navy Operational Global Analysis and Prediction System (NOGAPS) to study the 4 - 10 day disturbances over the eastern tropical Pacific. The period of study is May - September of 1989, 1990 and 1991. Spectral and cross-spectral analyses were used to determine the structure of the disturbances.

The results show zonal wavelengths of 3000 to 8000 kilometers and a tendency of northeast-southwest tilt in the meridional direction. The results show that 1991 appears to be the most active year, based on the highest relative variance in the 4 - 10 day window and the highest coherence between parameters.

The vertical tilt was found to be westward with height above 300 - 400 hpa in 1989 and above 200 hpa in 1990 and 1991. This interannual variation was consistent with the change in vertical shear of the mean zonal wind. Below 400 hpa in 1989 and 200 hpa in 1990 and 1991, the vertical tilt was eastward with height.

The thermal structure was consistent with the hydrostatic relationship in all three years. Waves transport heat equatorward below 200 hpa and poleward above 200 hpa.

20. DISTRIBUTION/AVAILABILITY OF ABSTRACT
☒ UNCLASSIFIED/UNLIMITED ☐ SAME AS REPORT ☐ DTIC USERS

21. ABSTRACT SECURITY CLASSIFICATION
UNCLASSIFIED

22a. NAME OF RESPONSIBLE INDIVIDUAL	22b. TELEPHONE *(Include Area code)*	22c. OFFICE SYMBOL
Chih-Pei Chang	(408) 656-2840	MR/Cp

DD FORM 1473, 84 MAR

83 APR edition may be used until exhausted
All other editions are obsolete

SECURITY CLASSIFICATION OF THIS PAGE
UNCLASSIFIED

Spectral Analysis of Synoptic Time Scale Disturbances Over the Tropical Eastern Pacific During Summer 1989, 1990 and 1991

by

William Christopher Swett
Lieutenant Commander, United States Navy
B.S., Jacksonville University, 1983

Submitted in partial fulfillment of the requirements for the degree of

MASTER OF SCIENCE IN METEOROLOGY AND PHYSICAL OCEANOGRAPHY

from the

NAVAL POSTGRADUATE SCHOOL
March 1993

Author: [redacted]
William Christopher Swett

Approved by: [redacted]
C. P. Chang, Co-Advisor

[redacted]
Tom Murphree, Co-Advisor

[redacted]
R. L. Haney, Chairman, Department of Meteorology

ABSTRACT

In this study we used data analyzed by the Navy Operational Global Analysis and Prediction System (NOGAPS) to study the 4 - 10 day disturbances over the eastern tropical Pacific. The period of study is May - September of 1989, 1990 and 1991. Spectral and cross-spectral analyses were used to determine the structure of the disturbances.

The results show zonal wavelengths of 3000 to 8000 kilometers and a tendency for northeast-southwest tilt in the meridional direction. The most active year appears to be 1991, with the highest relative variance in the 4 - 10 day window and the highest coherence between parameters.

The vertical tilt was found to be westward with height above 300 - 400 hpa in 1989 and above 200 hpa in 1990 and 1991. This interannual variation was consistent with the change in vertical shear of the mean zonal wind. Below 400 hpa in 1989 and 200 hpa in 1990 and 1991, the vertical tilt was eastward with height.

The thermal structure was consistent with the hydrostatic relationship in all three years. The waves transport heat poleward above 200 hpa and equatorward below 200 hpa.

TABLE OF CONTENTS

ACKNOWLEDGEMENTS

Many thanks to Professors Chih-Pei Chang and Tom Murphree for their advice and guidance. Their assistance was instrumental to the success of this research.

Thanks also to Professors J.M. Chen and Pat Harr of the Naval Postgraduate School and to Dr. Leong Chuan Quah of the Meteorological Service, Brunei for their much needed and appreciated software support.

This work was supported in part by the Naval Research Laboratory, Marine Meteorology Division, and by the National Science Foundation Grant ATM-9106495. The NOGAPS data were provided by the Fleet Numerical Weather Center.

I. INTRODUCTION

Observations of tropical waves have been very limited by a scarcity of observation stations. Early studies of tropical waves used time series from a few scattered observation stations to identify the basic structure, extent, and propagation characteristics of these waves (Yanai and Maruyama, 1966; Wallace and Chang, 1969; Chang et al., 1970). More recent studies in the western Pacific used model data from the European Center for Medium-range Weather Forecasts (ECMWF), verified by regional analyses produced by the Royal Observatory of Hong Kong (Lau and Lau, 1989) and by satellite outgoing longwave radiation (OLR) measurements (Liebmann and Hendon, 1990).

The tropical waves examined in these studies typically have wavelengths of about 2500-6000 kilometers, propagate westward at about 5-10 meters per second, transfer westerly momentum away from the equator, and have periods that are normally less than two weeks and may vary significantly with location. They have been identified primarily in the lower tropospheric meridional wind components and low level vorticity, but oscillations of this type are not limited to low levels or to these parameters.

Following the discovery of the quasi-biennial oscillation in the early 1960's, researchers (Reed, 1962; Tucker, 1964)

suggested that there might be a relationship between the changes in the stratospheric mean zonal wind and eddy transport of momentum toward the equator. Other researchers sought to identify and describe this eddy transport through spectral analysis of observations from tropical Pacific islands (Yanai and Maruyama, 1966; Yanai and Hayashi, 1969; Yanai and Murakami, 1970). These researchers noted a 4-5 day peak in the frequency spectrum of the meridional wind in the upper troposphere and lower stratosphere. The waves thus identified were found to have a horizontal wavelength of about 10,000 kilometers and a westward phase shift with height. Other studies (Rosenthal, 1965; Matsuno, 1966; Lindzen, 1967) identified these waves as mixed Rossby-gravity waves and follow-on research (Maruyama, 1968; Yanai and Hayashi, 1969) indicated that the waves transport westerly momentum upward and sensible heat poleward. Thus, the waves described by these studies may be important in describing the tropical general circulation and large scale oscillations.

Recent work (Lau and Lau, 1990; Liebmann and Hendon, 1990) covered the entire global tropics by using the numerical weather prediction-assimilated analysis. Most of this work confirmed previous studies in the central and eastern Pacific, though the eastern Pacific was not an area of focus by these investigators. They found that waves are not very active in these regions, possibly due to minimum convective activity or lack of upper air data.

Our study expands on previous research in several ways. First, we focus on the eastern Pacific, an area in which easterly waves have not yet been well documented. The vast majority of previous studies have concentrated on synoptic disturbances in the western Pacific, Atlantic (Reed et al., 1977), Caribbean (Riehl, 1948) and over North Africa (Burpee, 1972, 1974). In this study, we have applied these tested spectral techniques to a new region of interest.

Second, this analysis used the Navy Operational Global Analysis and Prediction System (NOGAPS) analyses, rather than the ECMWF analyses used in previous studies. Use of NOGAPS data allows us to make a preliminary evaluation of an additional data set for the study of tropical waves. This additional data should promote future research in which analyses are used to compensate for inadequate station coverage. Due to a major upgrade in the software for version 3.0 of NOGAPS in early 1989 (Hogan and Rosmond, 1991), only data generated subsequent to this software modification is used.

Third, we have divided the data by year, so as to be able to study inter-annual variations. Previous studies in the central and eastern Pacific combined data over several years.

We chose spectral analysis as an appropriate method for quantifying the temporal and spatial characteristics of these waves. Unlike quasi-mesoscale phenomena, such as typhoons, easterly waves have periods and wavelengths that lend

themselves to spectral analysis. Since very little is known over the eastern tropical Pacific, spectral analysis is an appropriate first step to look at the data.

We will describe the data sets and the statistical and spectral techniques used for these analyses in Chapter II. Chapters III, IV, V, and VI present results from the calculation of the variance and the cross-spectra of base series with surrounding grid points, grid point wind analyses at different pressure levels, and different parameters at each grid point. Finally, Chapter VII gives our summary and conclusions.

II. DATA AND ANALYSIS METHODS

The data used in this study were analyses generated by the Navy Operational Global Atmospheric Prediction System (NOGAPS) spectral forecast model, versions 3.1 and 3.2. The periods covered were 1 May - 30 September for the years 1989, 1990, and 1991. The data were provided by the Fleet Numerical Oceanographic Center (FNOC) in Monterey, California.

The NOGAPS data for this study contain 61 analysis parameters at 2.5° x 2.5° resolution over the entire globe. Values for each parameter were available for 0000Z and 1200Z daily at pressure levels of 1000, 925, 850, 700, 500, 400, 300, 250, 200, 150, and 100 hPa. A complete list of these is included in Table 1. Our study area was 20°S - 40°N, 50°W - 160°W. This area includes the tropical eastern Pacific, but is extended to the north and east in order to allow comparison with extratropical and Caribbean regions (Figure 1).

As some data records were missing from the tape archives, two persistence-based techniques were used to fill data gaps. First, all missing records were filled with data from the following 12-hour analysis, if available. In a few cases, persistence over more than a 12-hour period had to be assumed. Table 2 lists the persistence substitutions of data records in chronological order.

Table 1

TABLE OF ANALYSIS DATA BY SERIAL NUMBER AND PARAMETER

Ser. Number	Parameter
1.	OPERATIONAL SLP
2.	NOGAPS OI SLP ANALYSIS
3.	NOGAPS SURFACE AIR TEMP
4.	SST ANALYSIS
5.	SENSIBLE + LATENT HEAT FLUX
6.	LATENT HEAT FLUX
7.	SOLAR HEAT FLUX
8.	TOTAL HEAT FLUX
9.	MARINE WIND SURFACE ANAL (U-COMP)
10.	MARINE WIND SURFACE ANAL (V-COMP)
11.	NOGAPS 1000 HPA HEIGHT ANAL
12.	NOGAPS 1000 HPA TEMP
13.	NOGAPS 1000 HPA U-COMP ANAL
14.	NOGAPS 1000 HPA V-COMP ANAL
15.	1000 HPA DEW POINT DEPRESSION
16.	NOGAPS 925 HPA HEIGHT ANAL
17.	NOGAPS 925 HPA TEMP
18.	NOGAPS 925 HPA U-COMP ANAL
19.	NOGAPS 925 HPA V-COMP ANAL
20.	925 HPA DEW POINT DEPRESSION
21.	NOGAPS 850 HPA HEIGHT ANAL
22.	NOGAPS 850 HPA TEMP
23.	NOGAPS 850 HPA U-COMP ANAL
24.	NOGAPS 850 HPA V-COMP ANAL
25.	850 HPA DEW POINT DEPRESSION
26.	NOGAPS 700 HPA HEIGHT ANAL
27.	NOGAPS 700 HPA TEMP
28.	NOGAPS 700 HPA U-COMP ANAL
29.	NOGAPS 700 HPA V-COMP ANAL
30.	700 HPA DEW POINT DEPRESSION
31.	NOGAPS 500 HPA HEIGHT ANAL
32.	NOGAPS 500 HPA TEMP
33.	NOGAPS 500 HPA U-COMP ANAL
34.	NOGAPS 500 HPA V-COMP ANAL
35.	500 HPA DEW POINT DEPRESSION
36.	NOGAPS 400 HPA HEIGHT ANAL
37.	NOGAPS 400 HPA TEMP
38.	NOGAPS 400 HPA U-COMP ANAL
39.	NOGAPS 400 HPA V-COMP ANAL
40.	400 HPA DEW POINT DEPRESSION
41.	NOGAPS 300 HPA HEIGHT ANAL
42.	NOGAPS 300 HPA TEMP
43.	NOGAPS 300 HPA U-COMP ANAL

Table 1 (cont)

TABLE OF ANALYSIS DATA BY SERIAL NUMBER AND PARAMETER (CONT)

44.	NOGAPS 300 HPA V-COMP ANAL
45.	300 HPA DEW POINT DEPRESSION
46.	NOGAPS 250 HPA HEIGHT ANAL
47.	NOGAPS 250 HPA TEMP
48.	NOGAPS 250 HPA U-COMP ANAL
49.	NOGAPS 250 HPA V-COMP ANAL
50.	NOGAPS 200 HPA HEIGHT ANAL
51.	NOGAPS 200 HPA TEMP
52.	NOGAPS 200 HPA U-COMP ANAL
53.	NOGAPS 200 HPA V-COMP ANAL
54.	NOGAPS 150 HPA HEIGHT ANAL
55.	NOGAPS 150 HPA TEMP
56.	NOGAPS 150 HPA U-COMP ANAL
57.	NOGAPS 150 HPA V-COMP ANAL
58.	NOGAPS 100 HPA HEIGHT ANAL
59.	NOGAPS 100 HPA TEMP
60.	NOGAPS 100 HPA U-COMP ANAL
61.	NOGAPS 100 HPA V-COMP ANAL

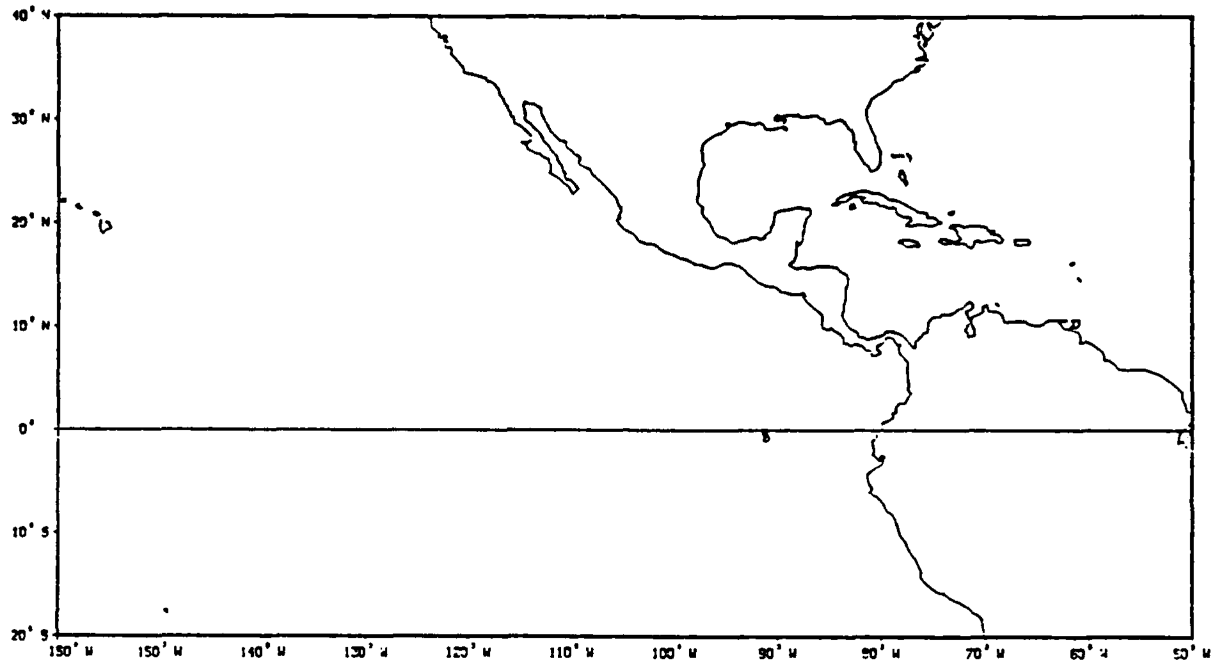

Figure 1: Map of study area

Table 2

TABLE OF MISSING DATA RECORDS AND PERSISTENCE SUBSTITUTIONS

Date	Parameter	Replacement
1 May 89	Marine Wind Surface Anal (V-comp) 00Z	+12hr
20 Jul 89	Solar Heat Flux 00Z	+12hr
25 Aug 89	Operational SLP 00Z	+12hr
28 Aug 89	Operational SLP 12Z	+12hr
27 May 90	Operational SLP 00Z	+12hr
13 Jul 90	Operational SLP 12Z	+12hr
17 Jul 90	Operational SLP 00Z	+12hr
24 Jul 90	Operational SLP 00Z	-12hr
	Operational SLP 12Z	+12hr
1 Sep 90	Latent Heat Flux 00Z	+12hr
13 May 91	1000 hPa V-comp Anal 00Z	+12hr
	500 hPa Temp 00Z	+12hr
	700 hPa Temp 12Z	+12hr
	300 hPa U-comp Anal 12Z	+12hr
14 May 91	500 hPa Temp 12Z	+12hr
	400 hPa Dew Point Depression 12Z	+12hr
15 May 91	Total Heat Flux 12Z	+12hr
16 May 91	300 hPa U-comp Anal 00Z	+12hr
	100 hPa Height Anal 00Z	+12hr
	500 hPa V-comp Anal 12Z	+12hr
17 May 91	300 hPa Temp 00Z	+12hr
18 May 91	500 hPa U-comp Anal 00Z	+12hr
	100 hPa Height Anal 00Z	+12hr
	300 hPa Height Anal 12Z	+12hr
	300 hPa U-comp Anal 12Z	+12hr
	250 hPa U-comp Anal 12Z	+12hr
19 May 91	850 hPa Temp 00Z	+12hr
	150 hPa Temp 00Z	+36hr
	150 hPa U-comp Anal 00Z	+24hr
	100 hPa U-comp Anal 00Z	+12hr
	850 hPa U-comp Anal 12Z	+12hr
	850 hPa Dew Point Depression 12Z	+12hr
	400 hPa U-comp Anal 12Z	+12hr
	200 hPa Temp 12Z	+12hr
	150 hPa Temp 12Z	+24hr
	150 hPa U-comp Anal 12Z	+12hr
20 May 91	Marine Wind Surface Anal (V-comp) 00Z	+12hr
	850 hPa Height Anal 00Z	+12hr
	700 hPa U-comp Anal 00Z	+12hr
	700 hPa Dew Point Depression 00Z	+12hr
	300 hPa U-comp Anal 00Z	+12hr
	150 hPa Temp 00Z	+12hr

Table 2 (cont)

TABLE OF MISSING DATA RECORDS (CONT)

Date	Parameter	Replacement
	200 hPa V-comp Anal 12Z	+24hr
	925 hPa Height Anal 12Z	+12hr
21 May 91	200 hPa U-comp Anal 00Z	+12hr
	200 hPa V-comp Anal 00Z	+12hr
22 May 91	500 hPa Temp 00Z	+12hr
	300 hPa Temp 00Z	+12hr
	500 hPa V-comp Anal 12Z	+12hr
23 May 91	500 hPa Height 12Z	+12hr
24 May 91	500 hPa Height 12Z	+12hr
	250 hPa U-comp Anal 12Z	+12hr
4 Jul 91	Latent Heat Flux 00Z	+12hr
29 Aug 91	Operational SLP 00Z	+12hr

Second, some records were present but were filled with dummy data (values of -1 for all grid points). In this case, a short subroutine in the co-spectrum analysis program tested for multiple occurrences of a -1 value within each record and filled missing data by persistence.

Analyses were carried out using the MVS subsystem of the Amdahl 5995-700A mainframe computer on the campus of the Naval Postgraduate School, Monterey, California. We modified a FORTRAN based programming package provided by Drs. L. C. Quah and J. M. Chen. We used modules from this package to load data from NOGAPS archive tapes to the MVS disk drives for random access, to display spectra of various parameters at individual grid points, to obtain plots of contribution to the variance of the selected spectral window, and to make co-variance plots of certain parameter pairs. We ran these FORTRAN modules as batch files on the MVS system and collected the outputs in graphic format on fanfold printouts.

We chose 200 hPa meridional wind as the key parameter for tracing waves in the upper troposphere and 850 hPa meridional wind for the lower troposphere. Meridional wind was expected to be clearer indicator of synoptic scale activity than zonal wind because zonal wind is associated with longer scales.

The power spectra indicated that the power in the 200 hPa and 850 hPa meridional winds for periods less than two weeks was not confined to a single frequency. Thus, we averaged the six spectral coefficients representing most of the power at

these time scales. These coefficients represent 4.0, 4.6, 5.3, 6.4, 8.0, and 10.6 day oscillations. The geographic distribution of the contributions to the variance were used to choose base series grid points for the spatial cross-spectral calculations.

Several different FORTRAN modules were used to calculate and plot cross-spectra. Two of these plot a single parameter base series along a given latitude or longitude against the same parameter at every other grid point on that parallel or meridian. This technique gave us a geographic plot for each parameter we considered. From this we made our observations of zonal wavelength and meridional tilt of waves in the meridional wind.

Another module plotted one parameter against another at every grid point in the domain, with one of the parameters undergoing comparison providing the base series for the other. This provided plots for inter-level and inter-parameter analyses. Only those plots which proved useful to the analysis are presented in this report.

For entry into the fast fourier transform, a 32-day lag period (64 lags) was used. The values obtained for the six spectral coefficients listed above were averaged, giving an estimated 34 degrees of freedom. This in turn gives a coherence squared at 98% confidence of about 0.17 or greater.

Additional modules and modifications of the modules above provided plots of mean or differenced values for various

parameters. Some of these plots were contoured while others were represented vectorially.

The graphic representation we chose for the cross-spectra data was a vector plot. Vector plots allowed us to combine phase difference and the magnitude of coherence squared into one graph. The phase difference averaging of the six frequencies was performed vectorially. In the vector plots, the vector direction represents the phase difference while the vector length represents the magnitude of the squared coherence. Clockwise rotation of vectors with respect to the vertical indicated base series lagging, while counter clockwise rotation indicated base series leading.

III. POWER SPECTRA

Figure 2 shows the power spectra of the meridional wind at 200 hPa (v200) at 5° x 5° grid resolution for the three years. The spectral peaks show considerable variations for different locations and different years. However significant variances can be observed at a majority of the grid points within the frequency window of (3 days)$^{-1}$ to (10 day)$^{-1}$, for all three years. This is true also for the meridional wind at 850 hPa (v850), whose power spectra (Figure 3) show even more concentrations within the synoptic frequency window. We therefore decided to average the data within the synoptic frequency window between periods 4 and 10.6 days to represent the synoptic time scale variations in the tropical eastern Pacific. The average period is 6.5 days.

Figure 4 shows the horizontal distribution of the absolute variances of v200 within the window for all three years. As expected, in both hemispheres the values are large only outside of the equatorial zone. This is due to the larger amplitude synoptic scale systems in the midlatitudes. The same is true at 850 hPa (Figure 5), however when relative variances (as a percentage of the total local variances) are plotted (Figure 6 for 200 hPa, and Figure 7 for 850 hPa), the tropical area is no less important within this synoptic window. It is particularly worth noting that, in addition to

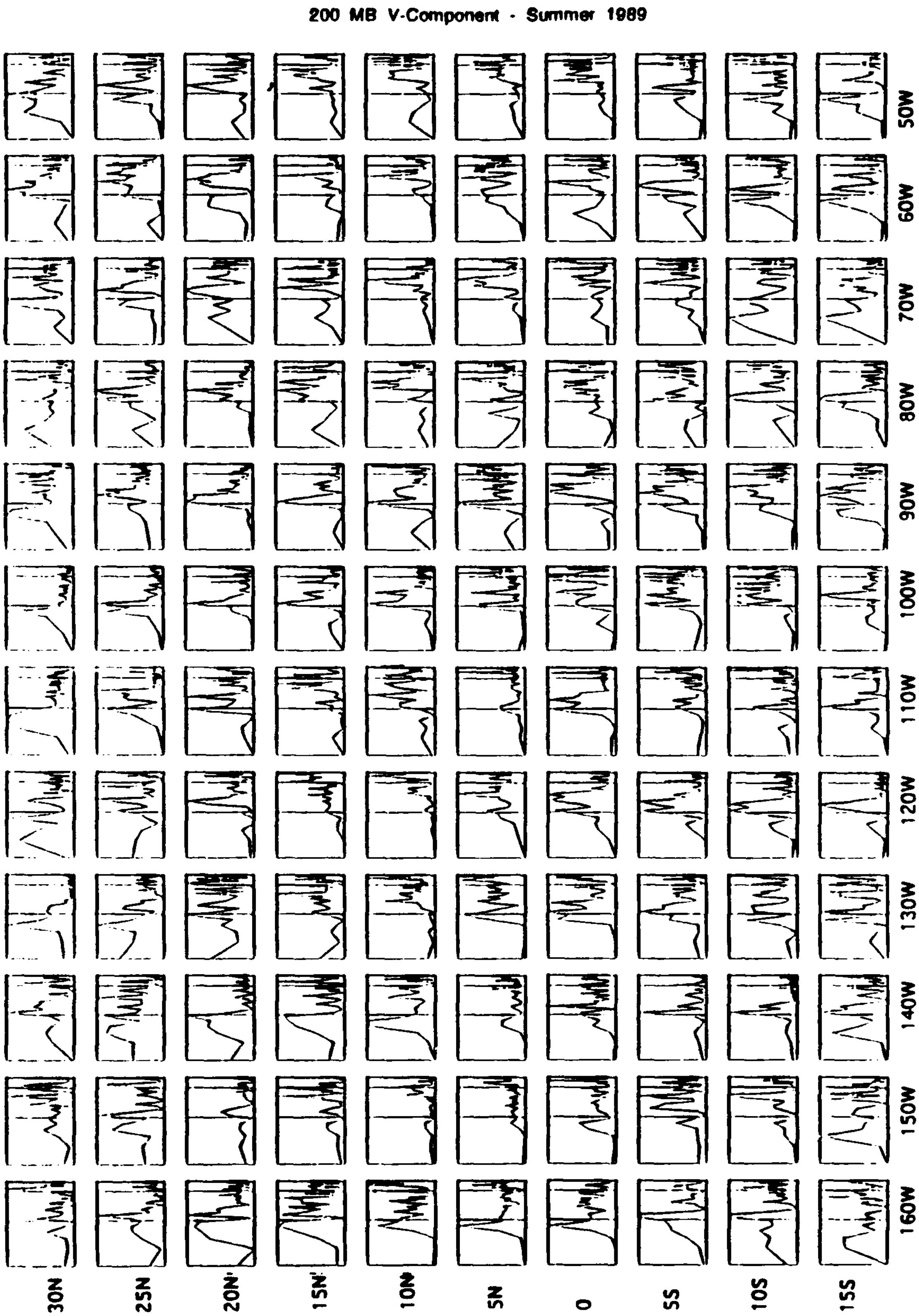

Figure 2a: Power spectra plots for gridpoints in 1989

200 MB V-Component - Summer 1990

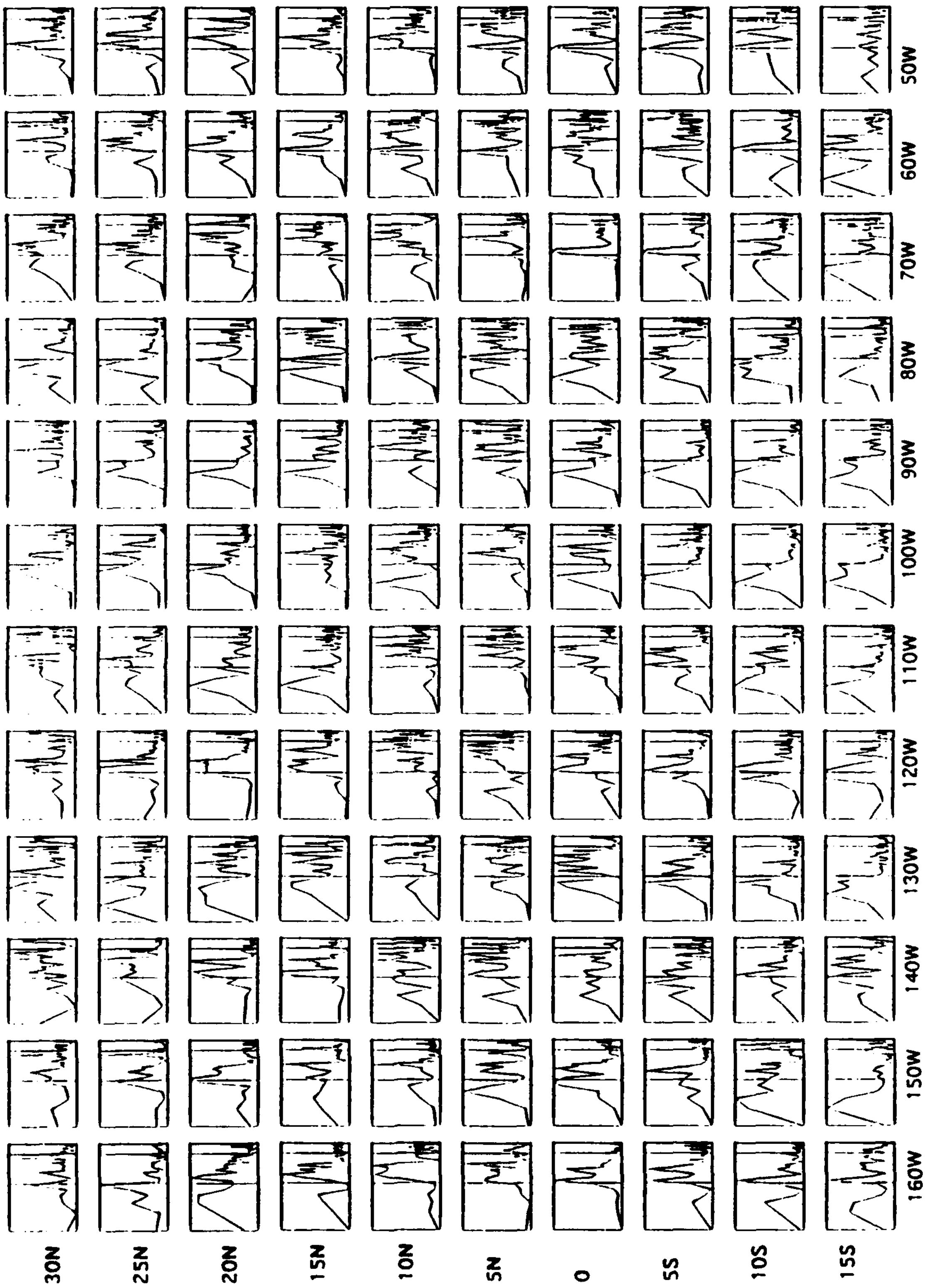

Figure 2b: Power spectra plots for gridpoints in 1990

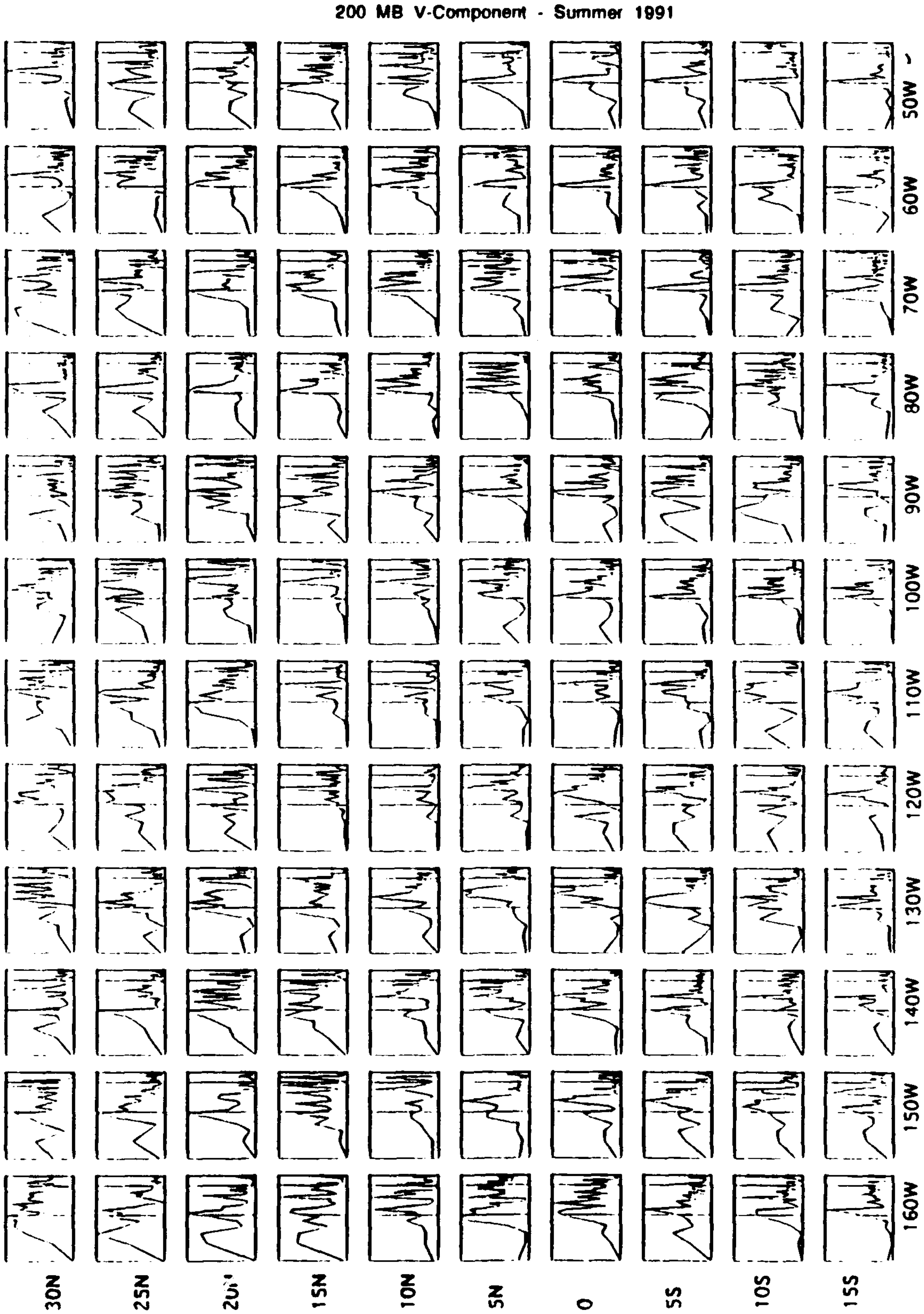

Figure 2c: Power spectra plots for gridpoints in 1991

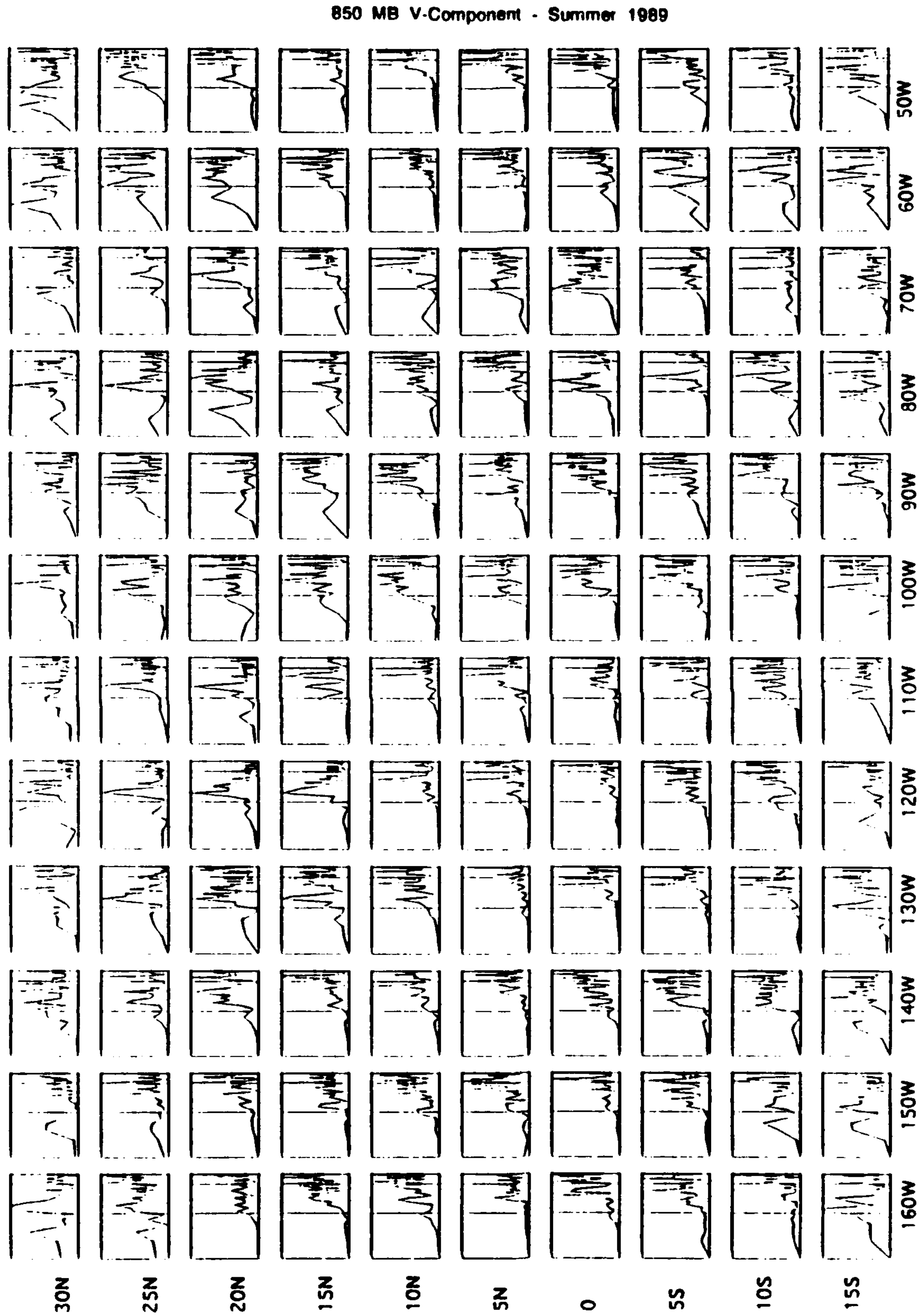

Figure 3a: Power spectra plots for gridpoints in 1989

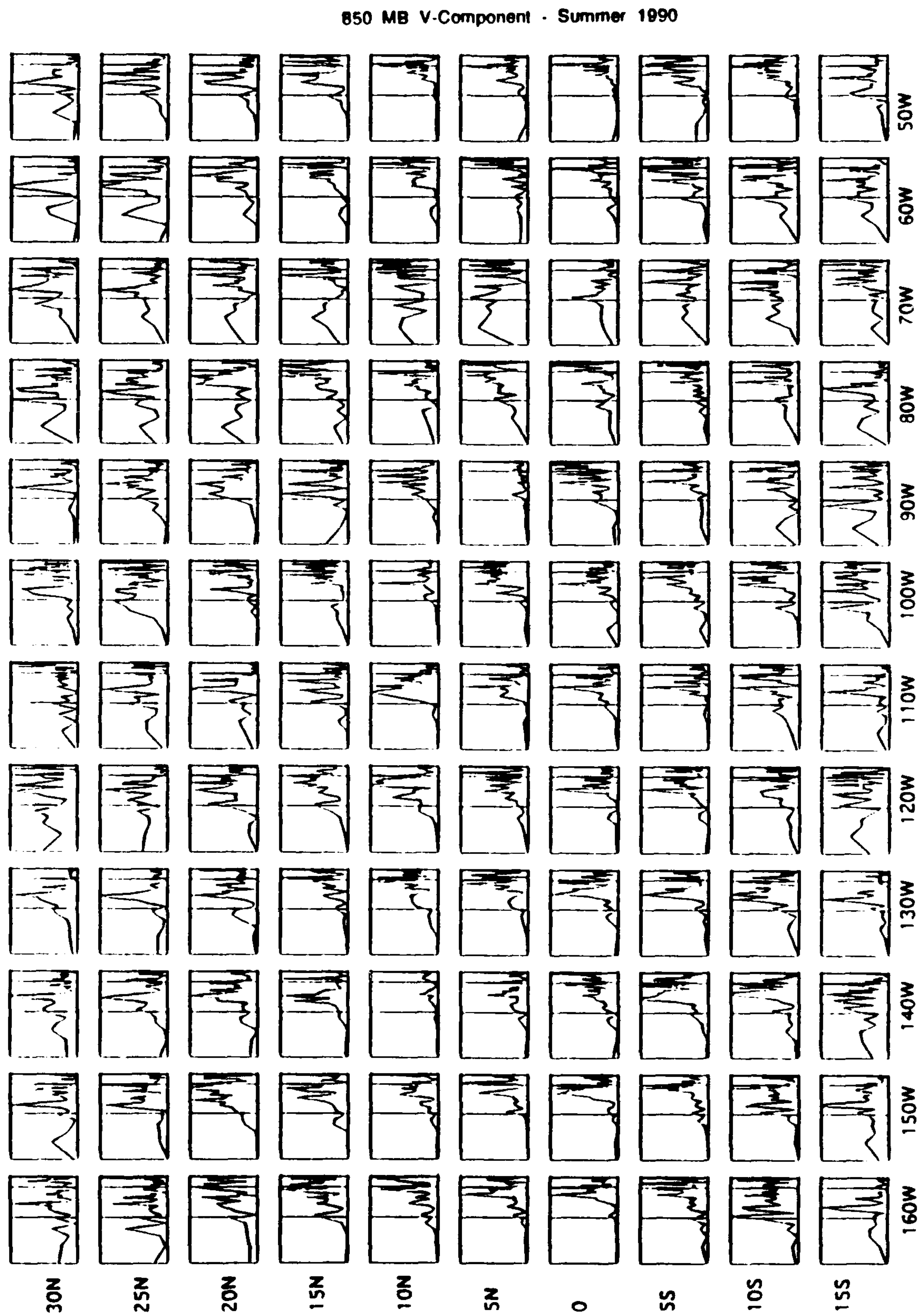

Figure 3b: Power spectra plots for gridpoints in 1990

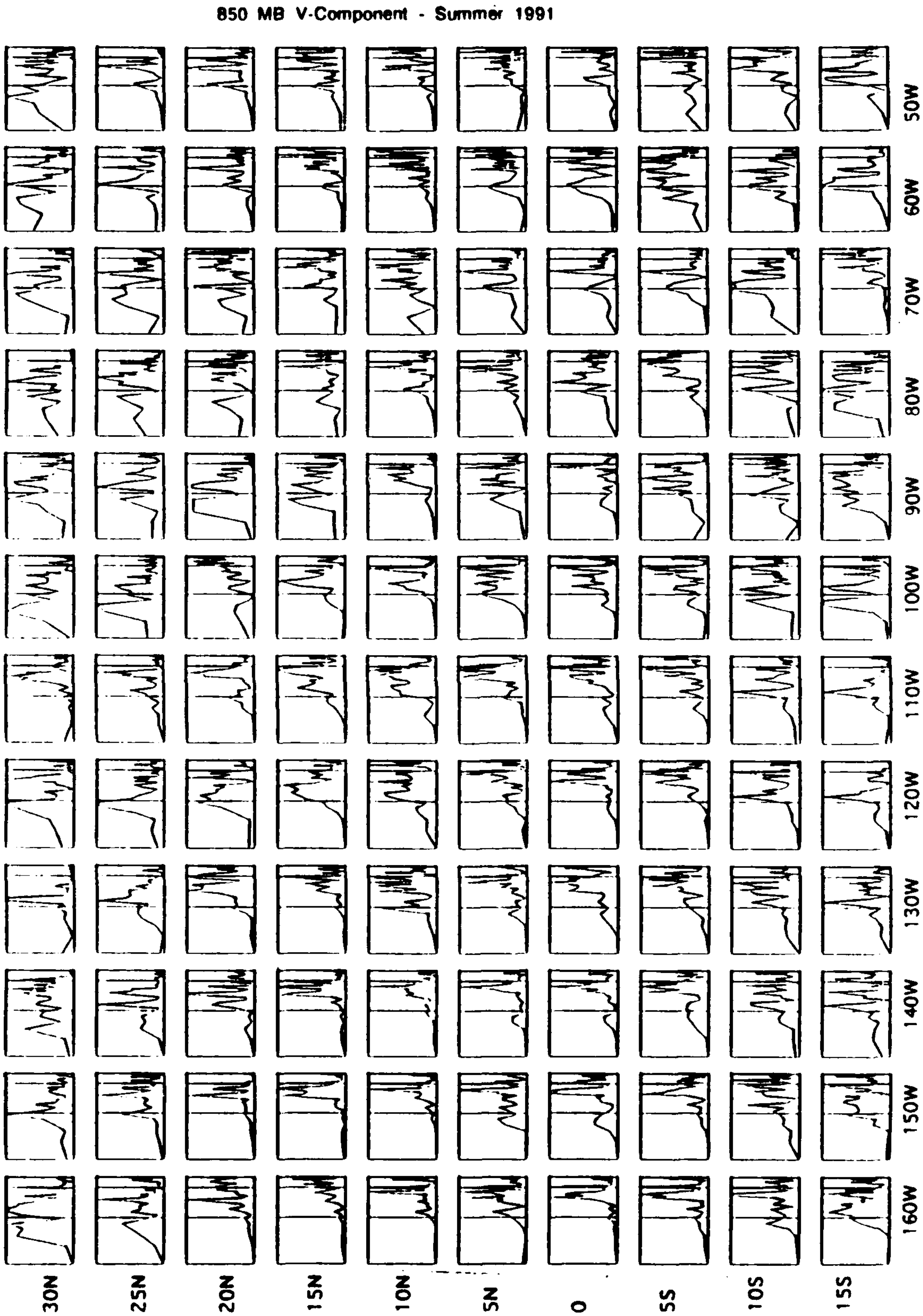

Figure 3c: Power spectra plots for gridpoints in 1991

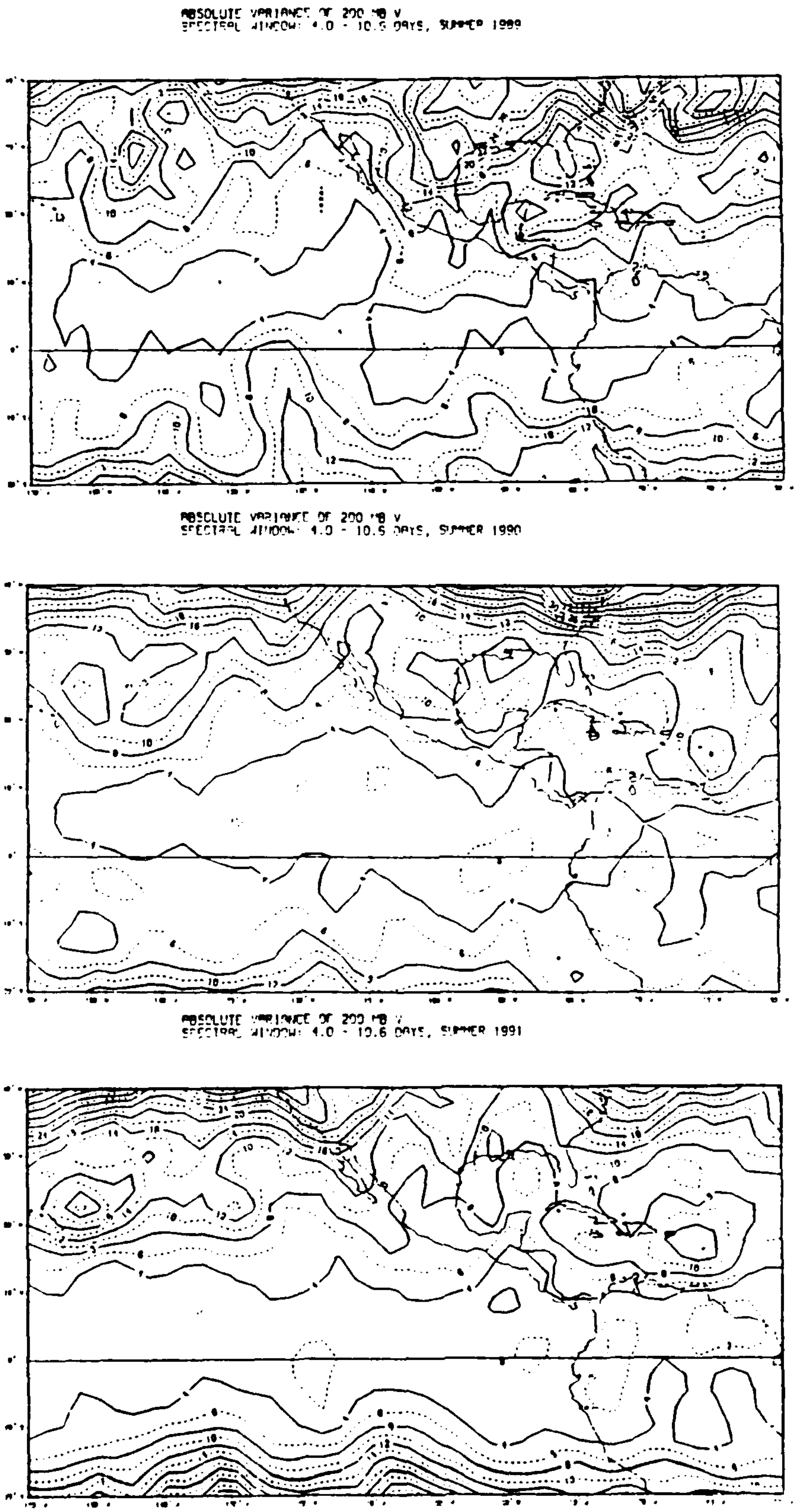

Figure 4a,b,c: Absolute variance of v200 in 1989, 1990, 1991

ABSOLUTE VARIANCE OF 850 MB V
SPECTRAL WINDOW: 4.0 - 10.6 DAYS, SUMMER 1989

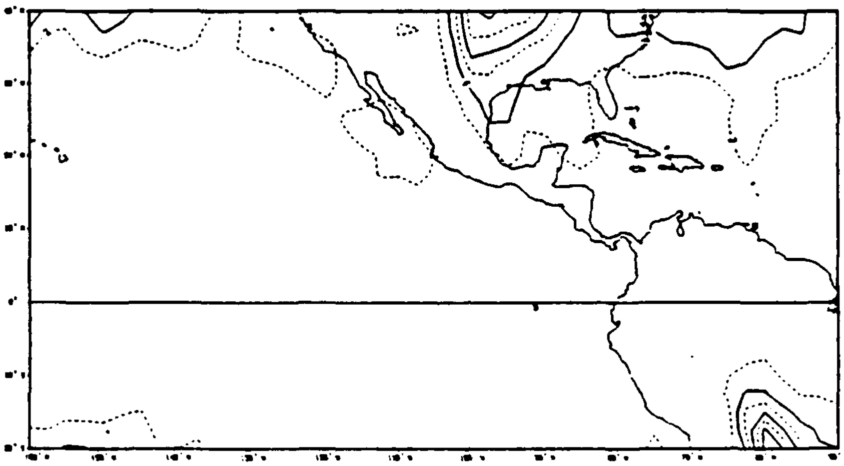

ABSOLUTE VARIANCE OF 850 MB V
SPECTRAL WINDOW: 4.0 - 10.6 DAYS, SUMMER 1990

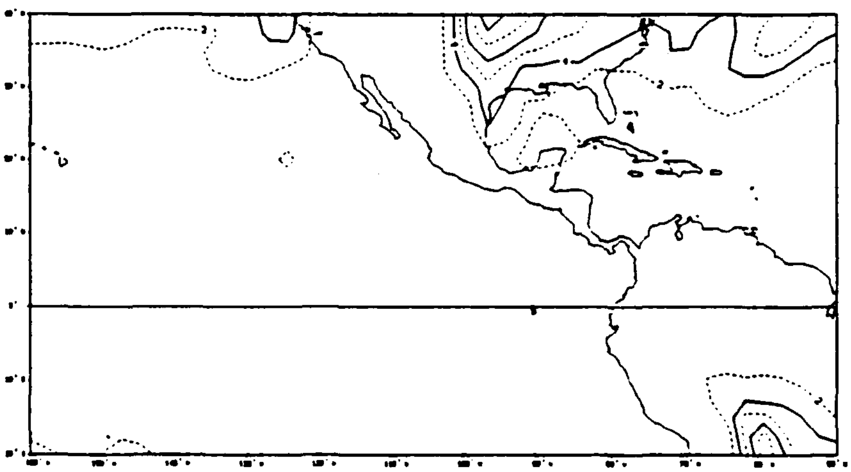

ABSOLUTE VARIANCE OF 850 MB V
SPECTRAL WINDOW: 4.0 - 10.6 DAYS, SUMMER 1991

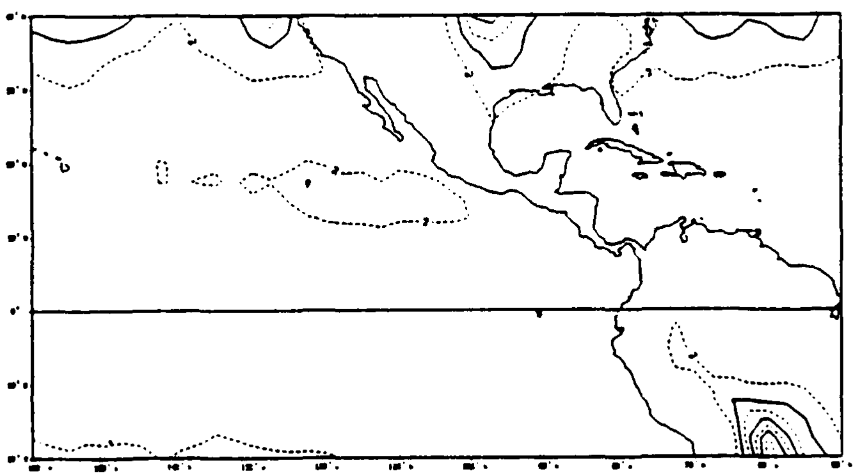

Figure 5a,b,c: Absolute variance of v850 in 1989, 1990, 1991

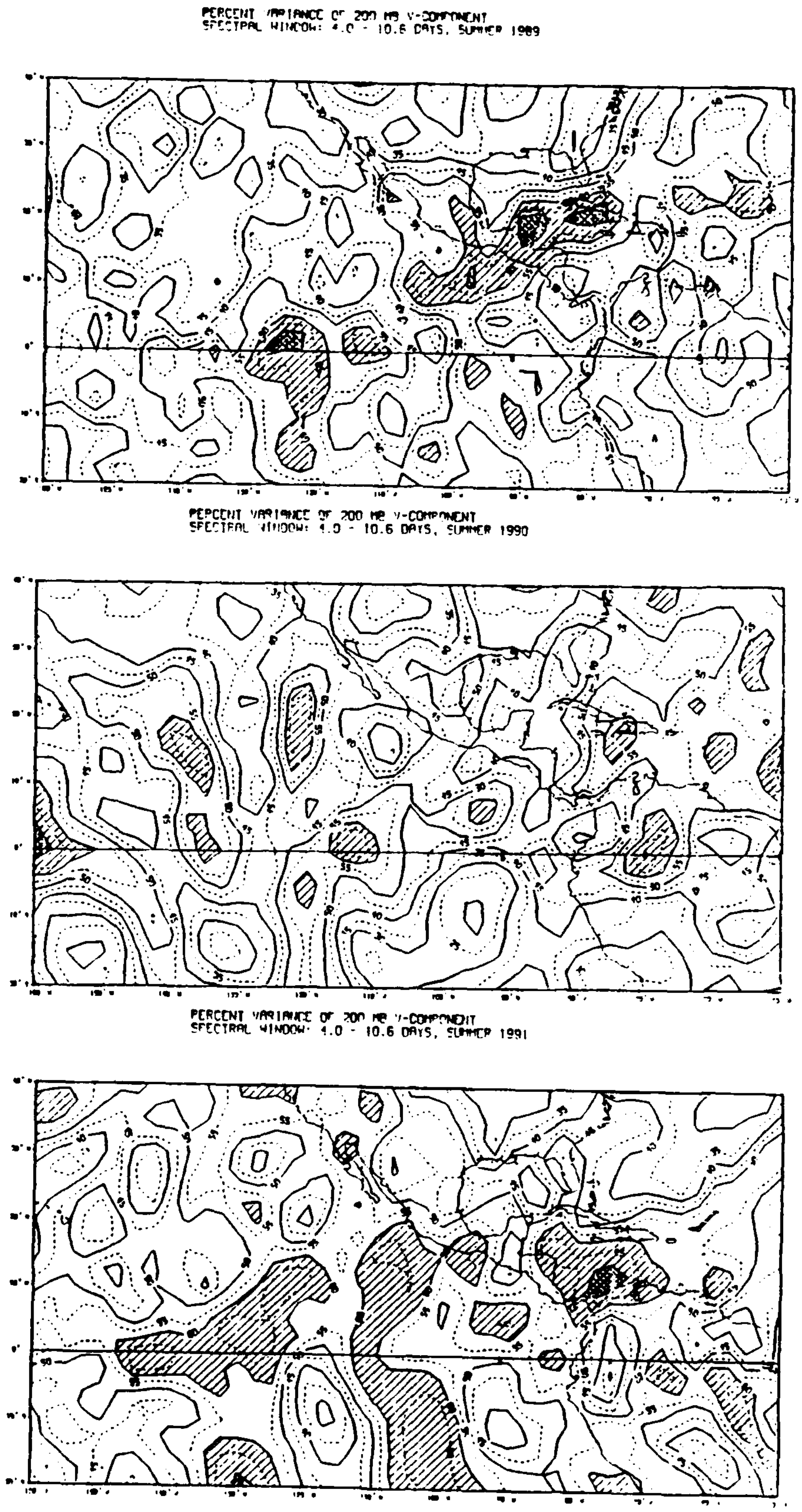

Figure 6a,b,c: Percent variance of v200 in 1989, 1990, 1991

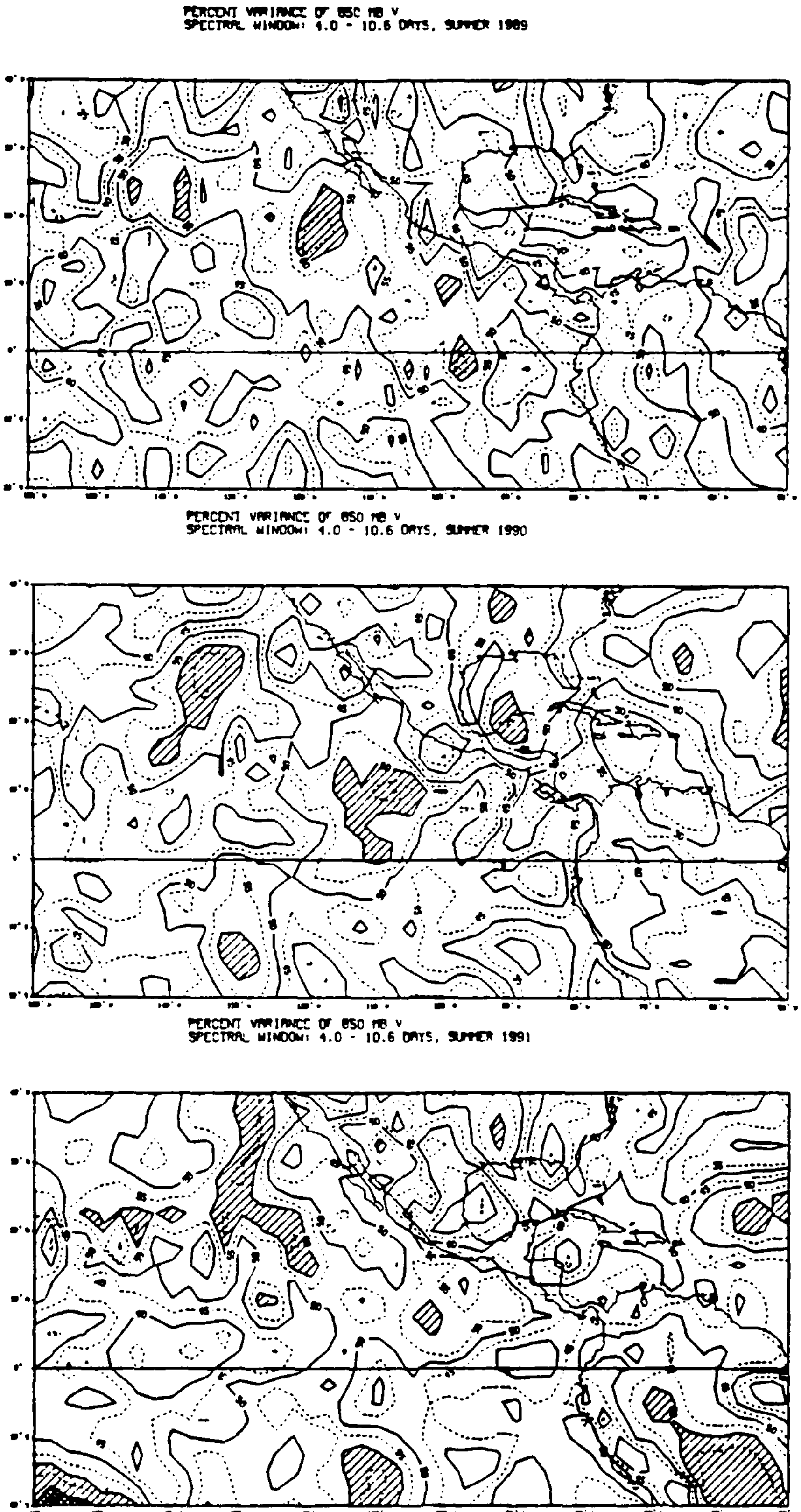

Figure 7a,b,c: Percent variance of v200 in 1989, 1990, 1991

the Caribbean Sea region where the classical easterly waves are known to exist (Riehl, 1948), the equatorial upper troposphere over the eastern Pacific also appears to be a very active region for the synoptic scale variations.

IV. HORIZONTAL STRUCTURE: CROSS-LONGITUDE (INTER-X) AND CROSS-LATITUDE (INTER-Y) CROSS-SPECTRA

The cross-spectra between v components at different longitudinal points along the same latitude were used to determine the zonal wavelength, and the cross-spectra between v components at different latitudinal points along the same longitude were used to determine the meridional structure. The former will be termed "inter-x" cross spectra and the latter "inter-y" cross spectra.

A. HORIZONTAL WAVELENGTH OF V AT 200 HPA

Figures 8 and 9 show the inter-x cross spectra for v200 for the three years, with the base longitude being 135°W, and 120°W, respectively. Here at each point the coherence squared and phase difference are represented by the length and direction of the vectors, respectively. A vector pointing northward means the oscillation at the point is perfectly in phase with that of the base point. A clockwise turning (positive phase difference) indicates that the base point lags, and a counter-clockwise turning indicates the base point leads.

All panels in Figures 8-9 show that, in the tropical region (20°S-20°N) the base point lags points immediately to the east and leads points immediately to the west. Thus the

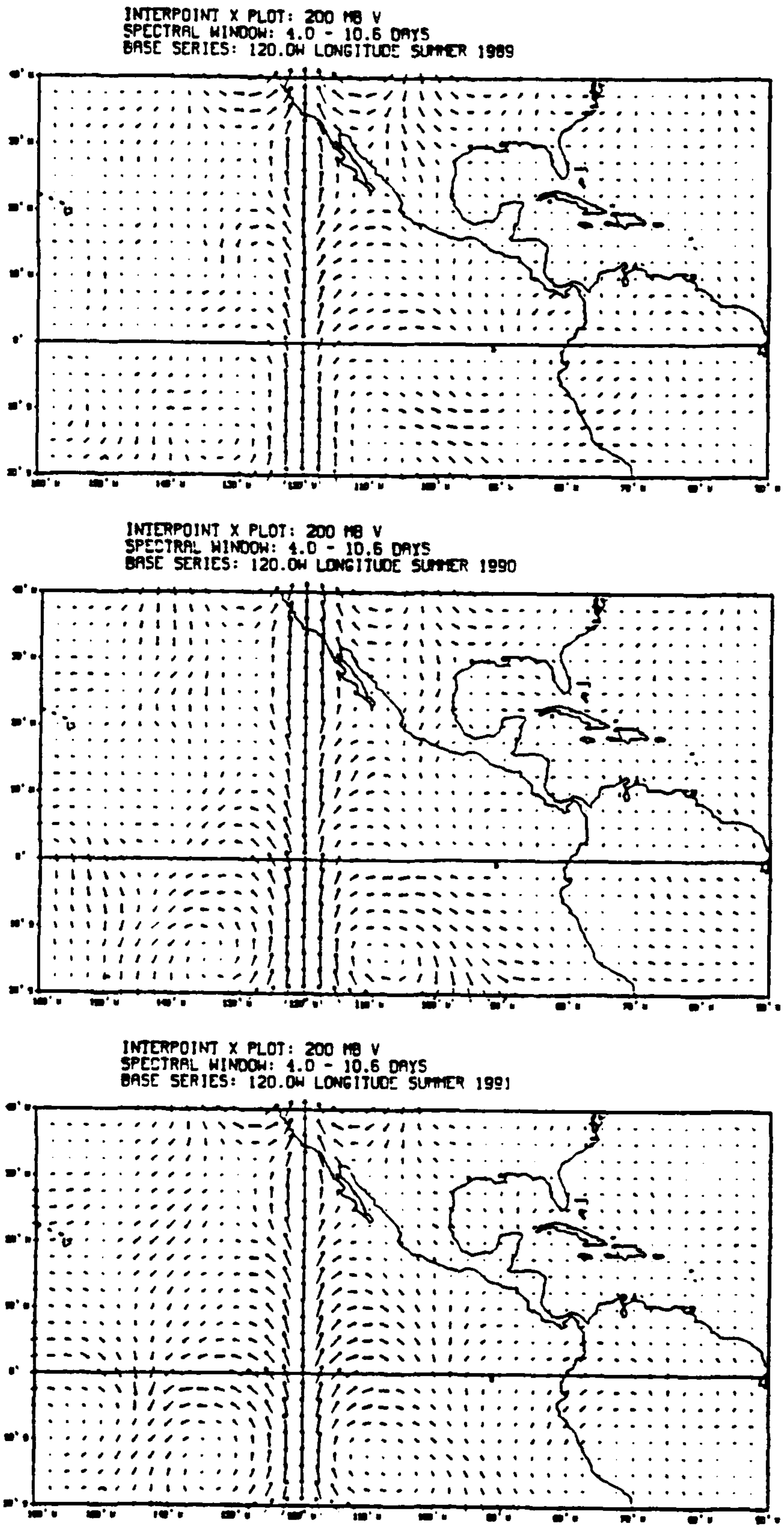

Figure 8a,b,c: Interpoint-x for v200 at 120°W in 1989, 1990, 1991

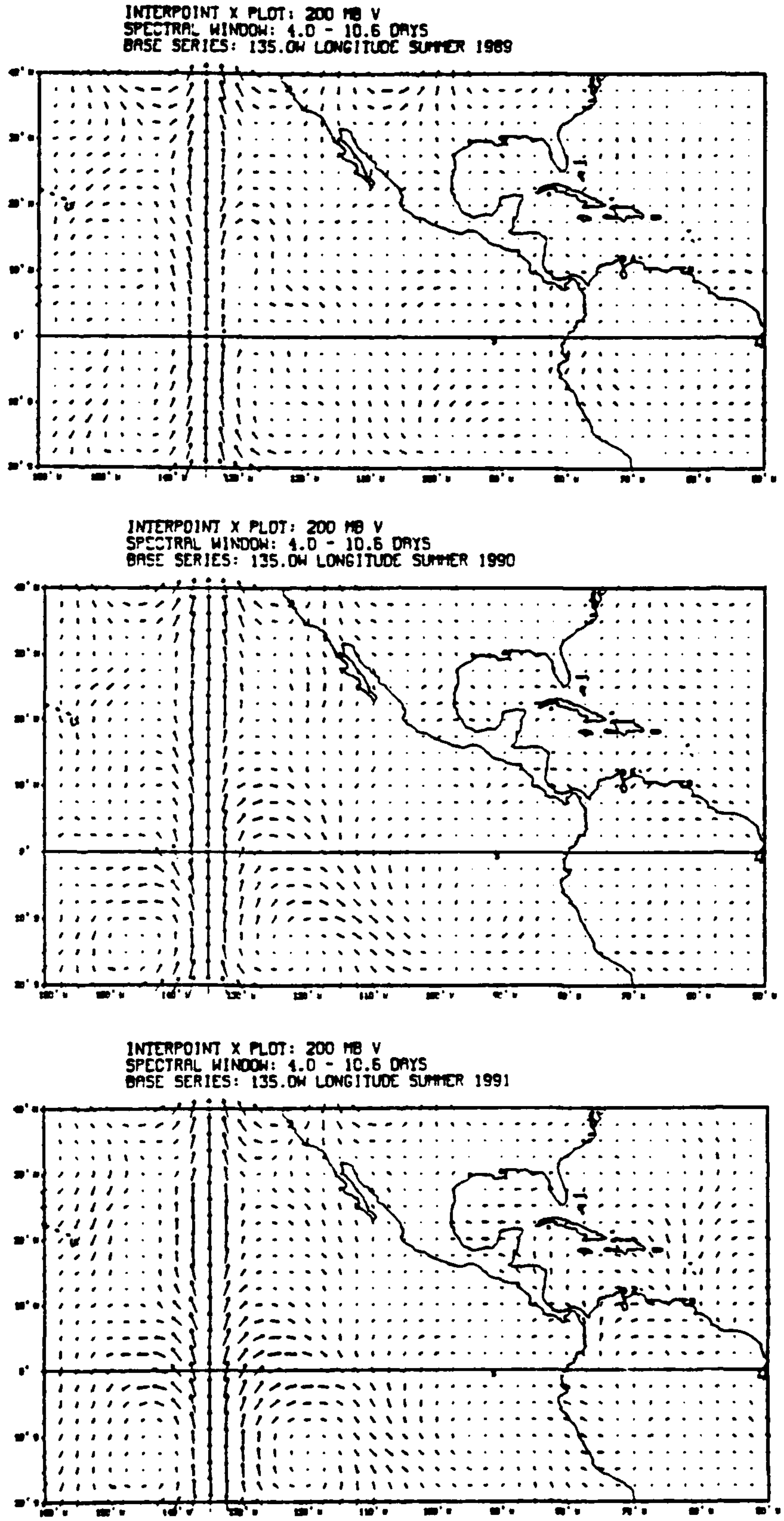

Figure 9a,b,c: Interpoint-x for v200 at 135°W in 1989, 1990, 1991

4-10 day fluctuations propagate from east to west. North of about 25°N the opposite is often true, indicating an eastward propagation in the northern midlatitudes.

From the zonal distance of a 180° phase shift we can determine the half-wavelength of the oscillations, if the coherence squared is significant (≥ 0.17 at the 98% level). By examining the phase shifts along three latitude bands centered at 15°N, equator, and 15°S in Figures 8 and 9, we constructed Table 3, which shows the wavelengths for the v200 field in different regions during each year.

Table 3

ZONAL WAVELENGTHS OF V200 IN KILOMETERS - LOW COHERENCE REGIONS OMITTED

			135°W	120°W
1989	15°N	5200	3000	4300
	0°	----	----	5400
	15°S	3200	5000	----
1990	15°N	3800	3200	3500
	0°	6000	5300	7000
	15°S	2700	3200	2700
1991	15°N	3000	5600	4300
	0°	5400	5600	4900
	15°S	2200	3800	3600

Inter-longitude v200 for 1991 in the northern tropics and equatorial belt has larger coherence squared than other years. In general, wavelengths are shorter in the northern and southern tropics and longer in the equatorial belt.

B. MERIDIONAL TILT OF V AT 200 HPA

Figure 10 shows the inter-y cross spectra for v200 for the three years, with the base points along 15°N. In general it can be seen that the base latitude lags points to the south and leads points to the north. Thus the disturbances have a northeast-southwest tilt around 15°N. However, during 1991 near the western end of our domain (central Pacific) there is a slight indication of the opposite tilt. The coherence squares are again larger in 1990 and 1991, indicating a better organization than 1989. It may be noteworthy that while there is almost no meridional tilt in the Caribbean Sea for all three years, the coherence and tilt in the subtropical western North Atlantic north of the Caribbean Sea are both prominent in 1989 and, to a slightly lesser degree, in 1991. These are areas of the classical easterly waves.

Figure 11 shows the inter-y cross-spectra for v200 for the three years, with the equator as the base latitude points. Here it can be seen that in the vicinity of the equator the meridional tilt is very slight. North of 7.5°N the tilt is consistent with the northeast-southwest tilt revealed in Figure 10. In the southern hemisphere the cross-spectra phase differences vary considerably, casting doubt on the usefulness of the southern hemisphere data.

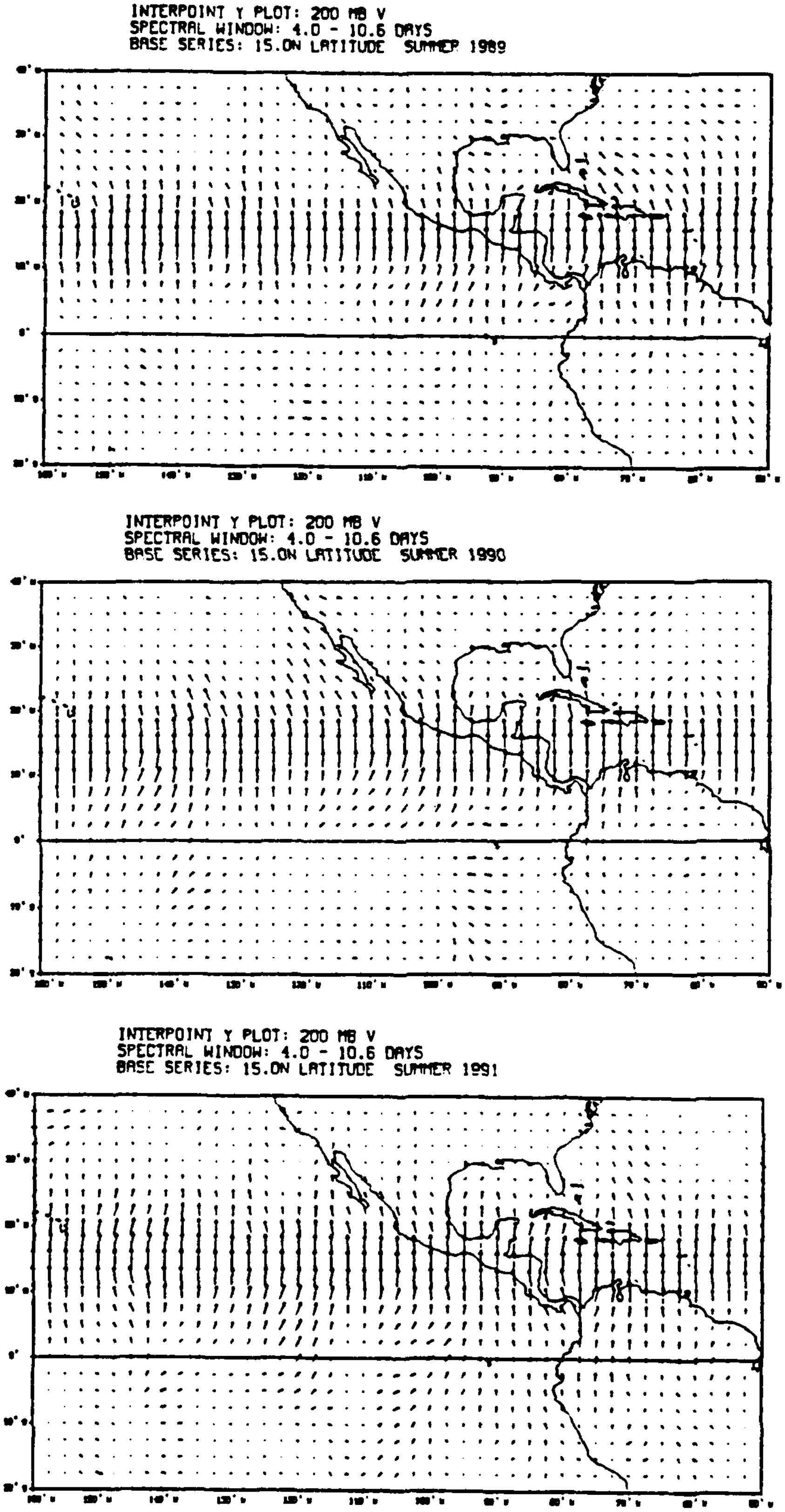

Figure 10a,b,c: Interpoint-y for v200 at 15°N in 1989, 1990, 1991

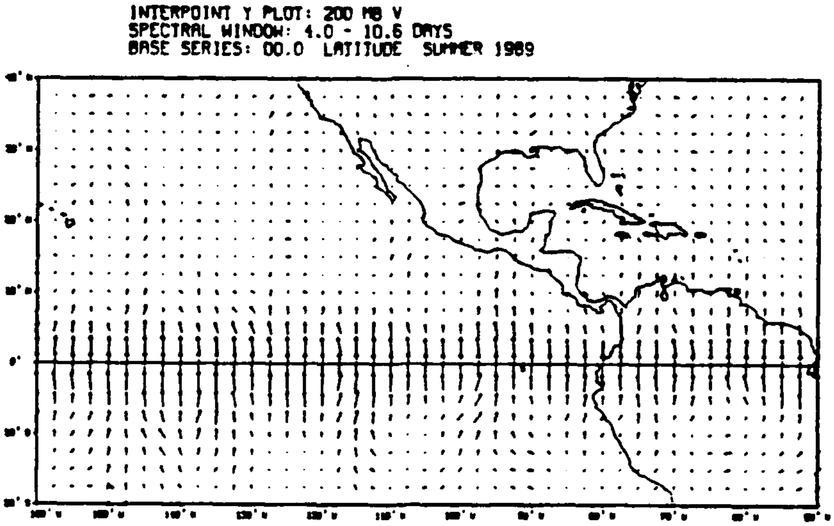

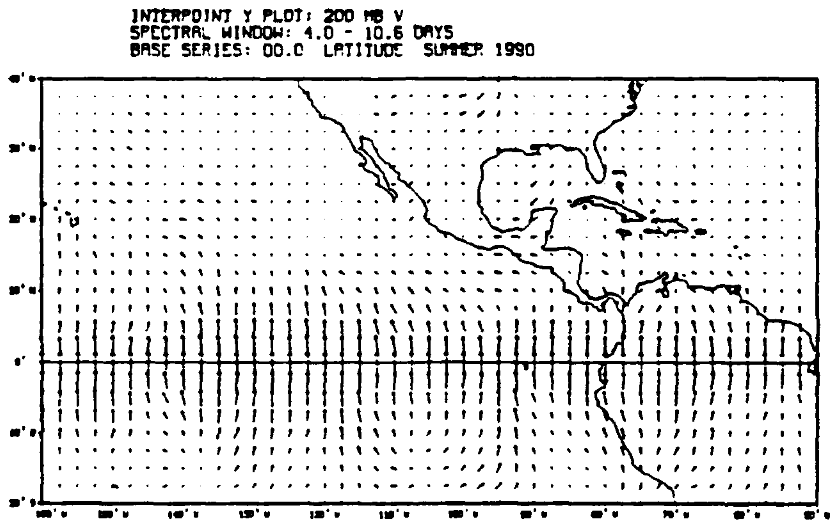

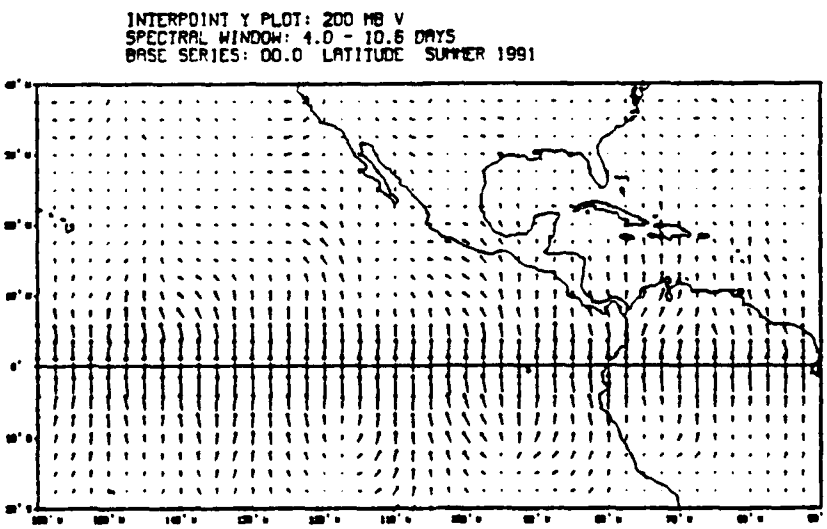

Figure 11a,b,c: Interpoint-y for v200 at 0° in 1989, 1990, 1991

C. HORIZONTAL WAVELENGTH OF V AT 850 HPA

As at 200 hPa, the horizontal wavelength of the v component at 850 hPa is determined from the inter-x cross spectra with two base longitudes: 120°W (*Figure 12*) and 135°W (Figure 13). In general, the disturbances propagate from east to west, as at 200 hPa. The interannual variation in the organization of the disturbances observed at 200 hPa are only slightly evident at 850 hPa. For both basic longitudes the inter-x coherence squares for 1989 are slightly smaller than other years at latitudes immediately north of the equator, although the difference is not large. On the other hand, Figure 12 shows that the 1989 v850 has more substantial coherence squared values than the other two years, indicating a short wave structure north of 20°N, with a half-wavelength reversal between 120°W and 140°W.

Table 4

ZONAL WAVELENGTHS OF V850 IN KILOMETERS - LOW COHERENCE REGIONS OMITTED

		135°W	120°W	
1989	15°N	2900	4000	2900
	0°	8000	6200	5200
	15°S	----	----	2800
1990	15°N	2400	2500	3100
	0°	7600	7000	7600
	15°S	5200	4200	6000
1991	15°N	4000	4200	2500
	0°	8000	6900	6400
	15°S	4300	4300	5400

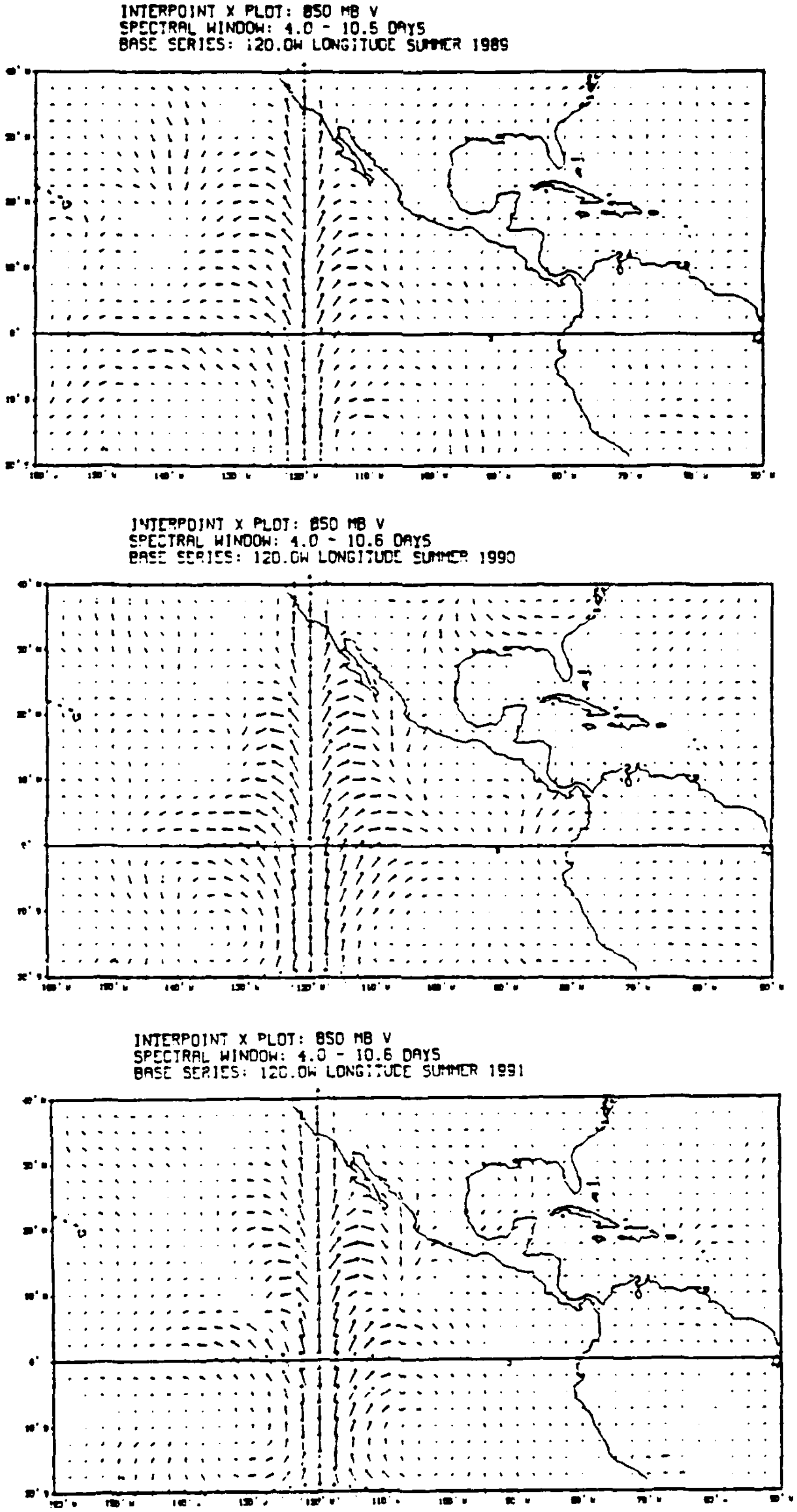

Figure 12a,b,c: Interpoint-x for v850 at 120°W in 1989, 1990, 1991

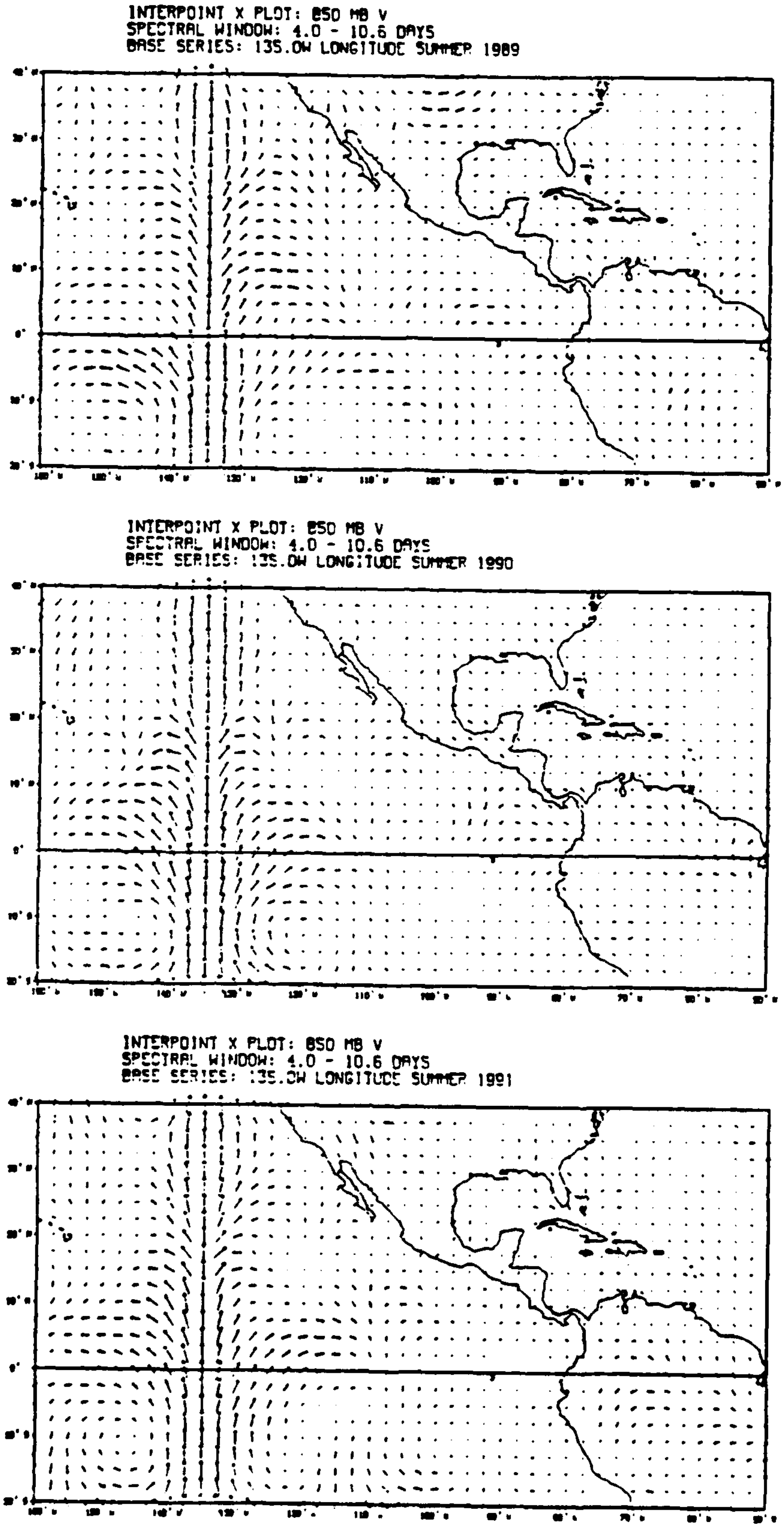

Figure 13a,b,c: Interpoint-x for v850 at 135°W in 1989, 1990, 1991

In the northern tropics the wavelengths are around 3000-4000 km, similar to 200 hPa. Equatorial belt wavelength is long: 6000-7000 km or more, also similar to 200 hPa. The southern tropics (15°S) have a slightly shorter wavelength than the equatorial values. Further south there are indications of short waves.

D. MERIDIONAL TILT OF V AT 850 HPA

Figures 14 and 15 show the inter-y cross spectra for v850 for the three years, with 15°N and the equator as the base latitudes, respectively. Figure 14 indicates a northeast-southwest tilt in the northern tropics for all three years, as at 200 hPa (Figure 10). In the equatorial zone, Figure 15 indicates that a similar tilt also exists in 1990, and to a much less extent in 1989 and 1991. In the southern tropics the phase tilt is again inconclusive.

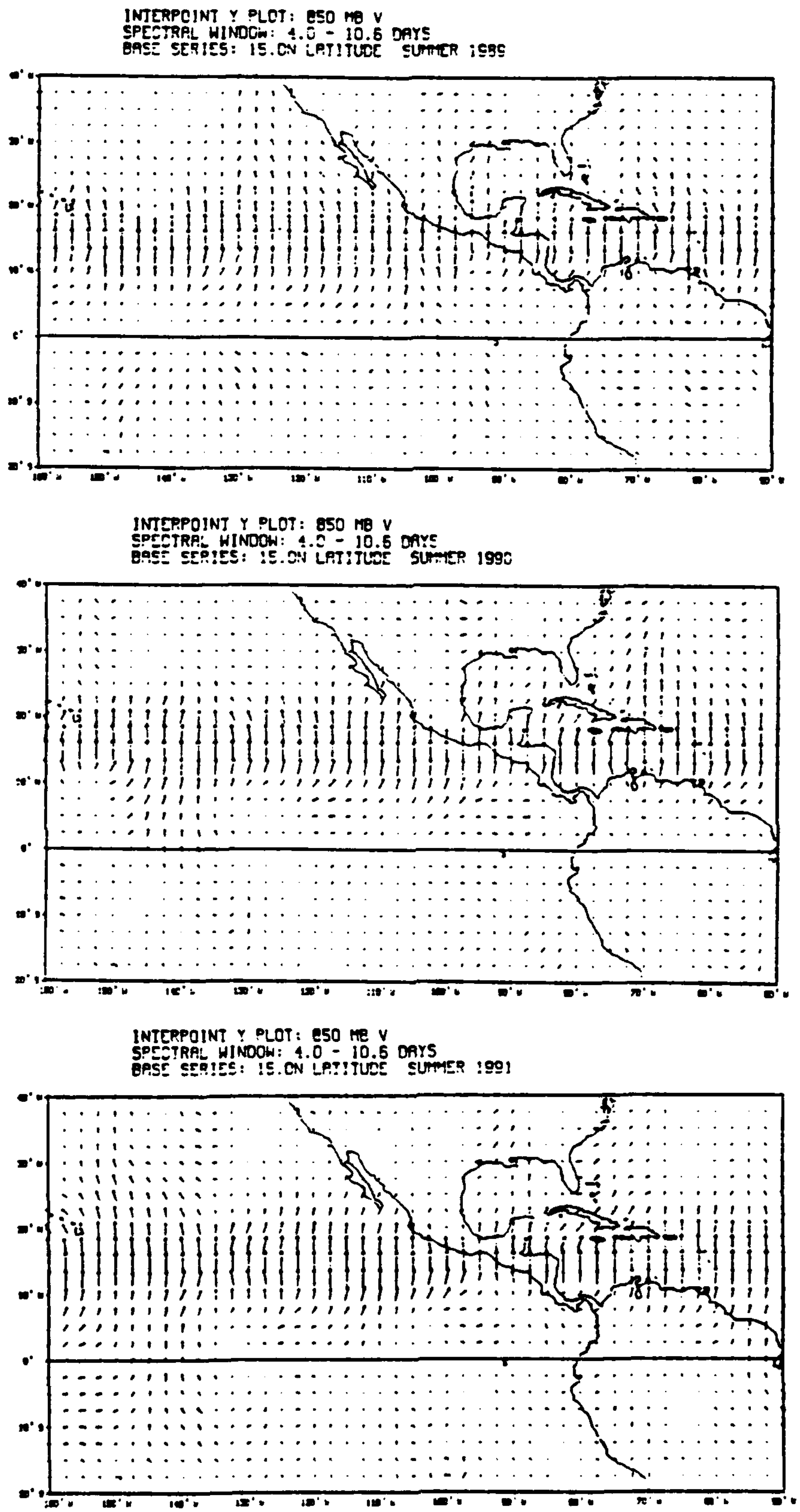

Figure 14a,b,c: Interpoint-y for v850 at 15°N in 1989, 1990, 1991

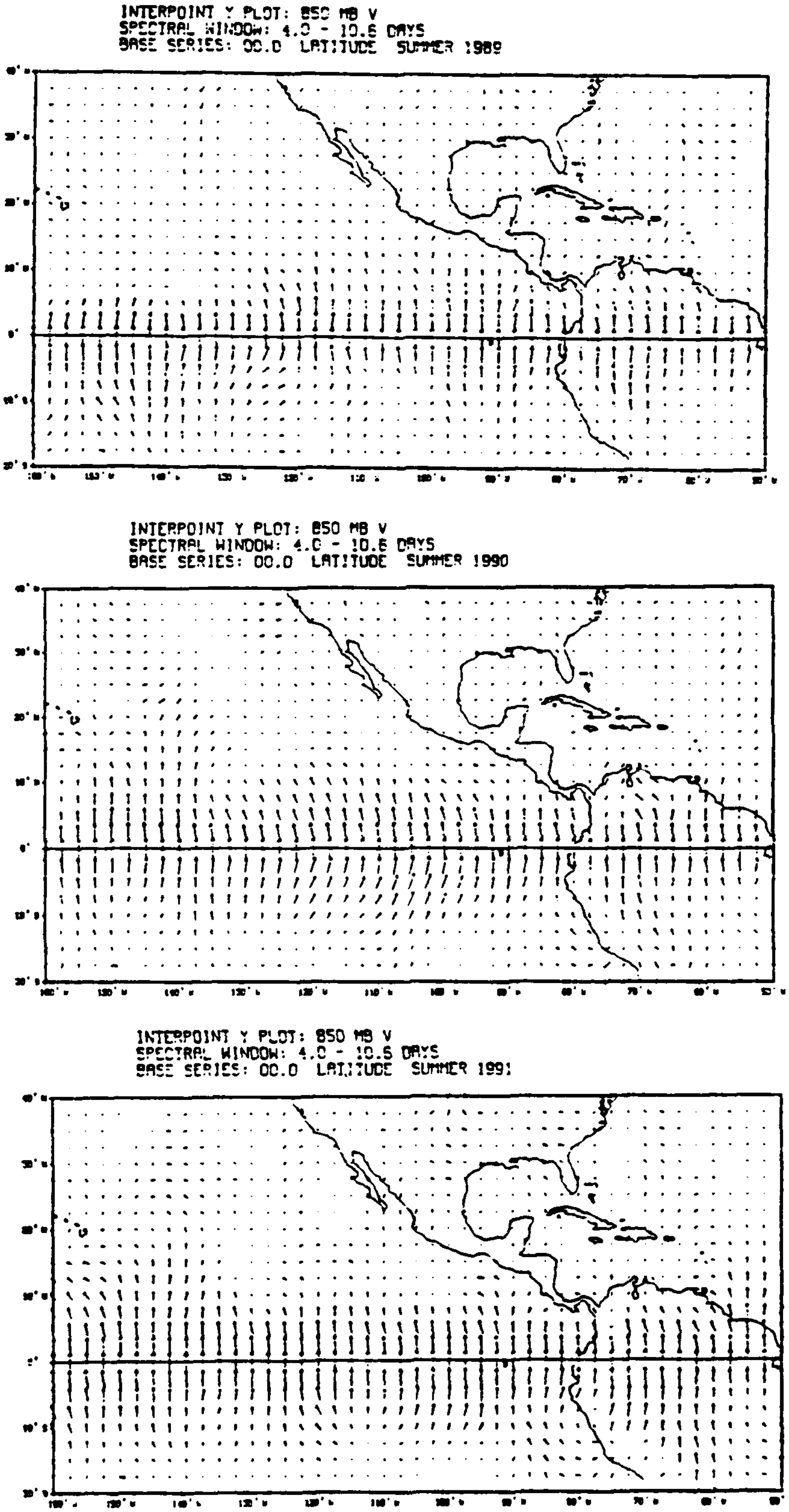

Figure 15a,b,c: Interpoint-y for v850 at 0° in 1989, 1990, 1991

V. VERTICAL STRUCTURE: INTER-LEVEL CROSS-SPECTRA

A. UPPER TROPOSPHERIC VERTICAL STRUCTURE

The upper tropospheric vertical structure based on the v component is determined by the cross-spectra between v at 200 hPa and six other levels: 100 hPa, 150 hPa, 300 hPa, 400 hPa, 500 hPa, and 700 hPa. The coherence squares and phase differences between v200, the base series, and v at each of these levels are shown in Figure 16 for the 20°N-20°S band. Since the disturbances are propagating westward, for levels below 200 hPa a positive phase difference (vector turning clockwise) indicates an eastward tilt with height, and a negative phase difference (vector turning counter-clockwise) indicates a westward tilt with height. Thus the vertical tilt can be visualized by following the direction of the phase vectors towards the top of the diagram. For levels above the base series v200, the opposite is true.

Figure 16a indicates that during 1989 the averaged vertical tilt is westward with height from 200 hPa to 100 hPa over the tropical eastern Pacific. The averaged phase difference is < 30° except near central America. Between 300 hPa and 200 hPa, the averaged vertical tilt is also westward within 10° of the equator. At 400 hPa the averaged tilt becomes eastward with height. Below 400 hPa the coherence squared in the equatorial zone rapidly decreases to below the

98% significance level, although closer inspection reveals a tendency toward continuous eastward tilt with height near the equator at the 500 hPa level.

Figures 16b and 16c show that 1990 and 1991 have similar vertical structures in the middle-upper troposphere. Between 200 hPa and 100 hPa, the vertical tilt is westward with height, the same direction as in 1989. However the phase differences are typically larger, often reaching 45° over a large part of the equatorial eastern Pacific in 1990, and even more so in 1991. The 1991 coherence between these two levels is the highest of the three years. Below 200 hPa both years show a consistent and continuous eastward tilt with height that can be traced down to 500 hPa with significant coherence. The phase change is near 90° between 500 hPa and 200 hPa, and in 1991 it exceeds 90° off the west coast of equatorial South America.

Figure 17 summarizes the middle-upper tropospheric vertical tilt for the three years. While for all cases the waves tilt westward with height in the upper troposphere above 200 hPa, there are considerable differences between 1989 and 1990-1991. In 1989 the westward tilt is weaker but it persists in the 300-200 hPa layer. In 1990-1991 the westward tilt is stronger between 200-100 hPa, but the tilt is eastward with height between 300-200 hPa. Below 300 hPa, all years show a tendency toward eastward tilt with height, with the 1989 signal being very weak and the 1990-1991

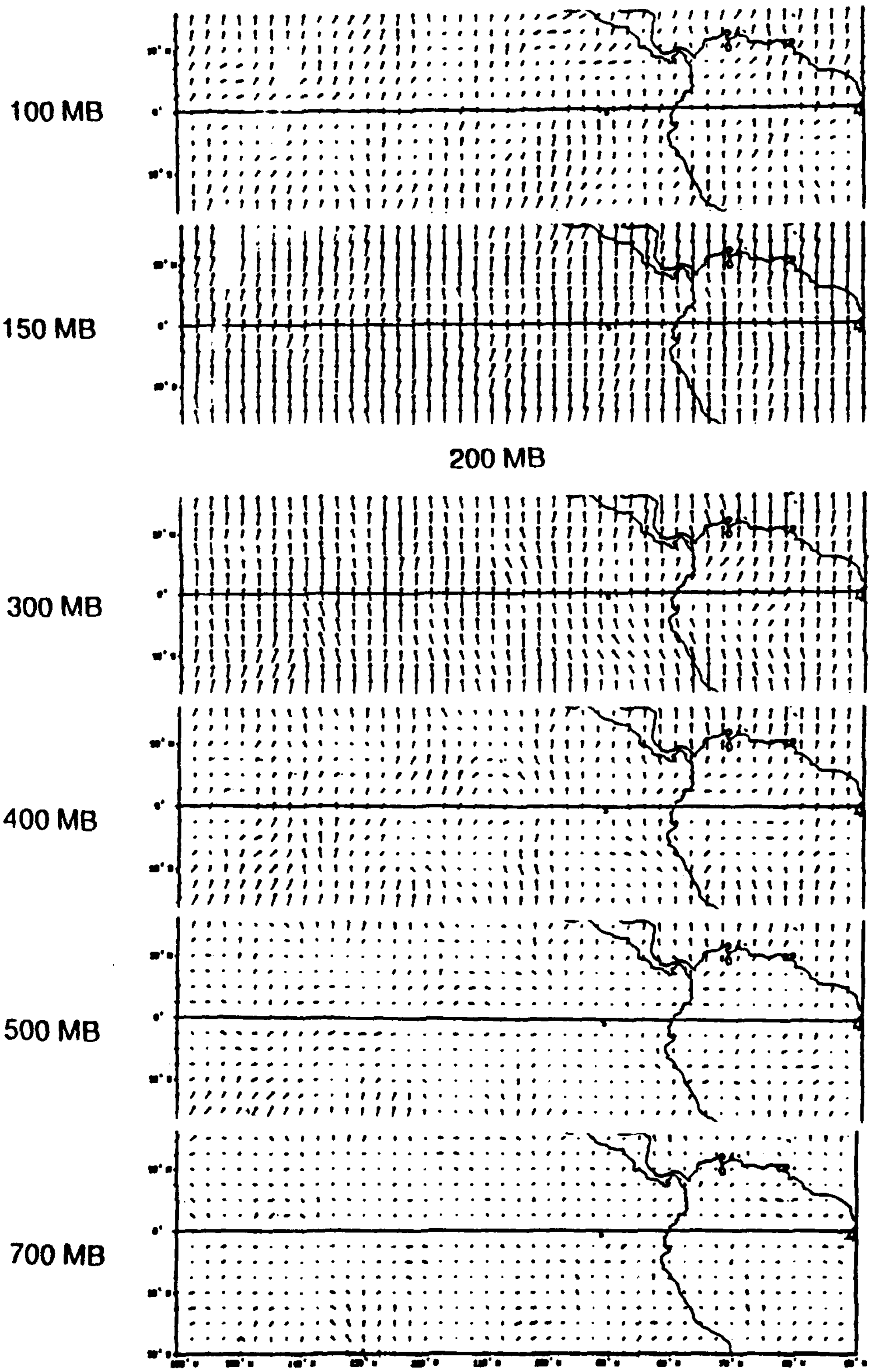

Figure 16a: Interlevel v200 comparison graph for 1989

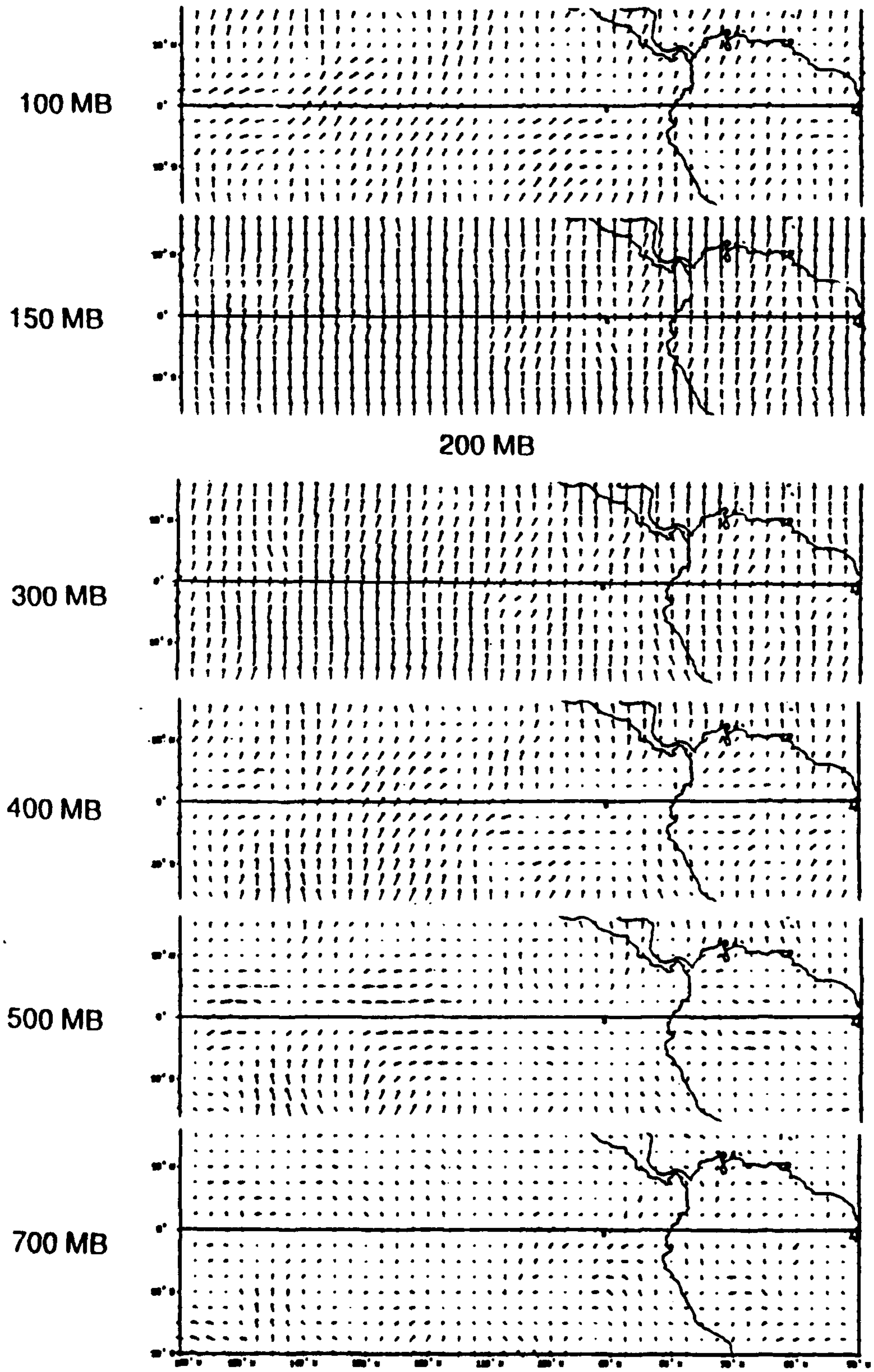

Figure 16b: Interlevel v200 comparison graph for 1990

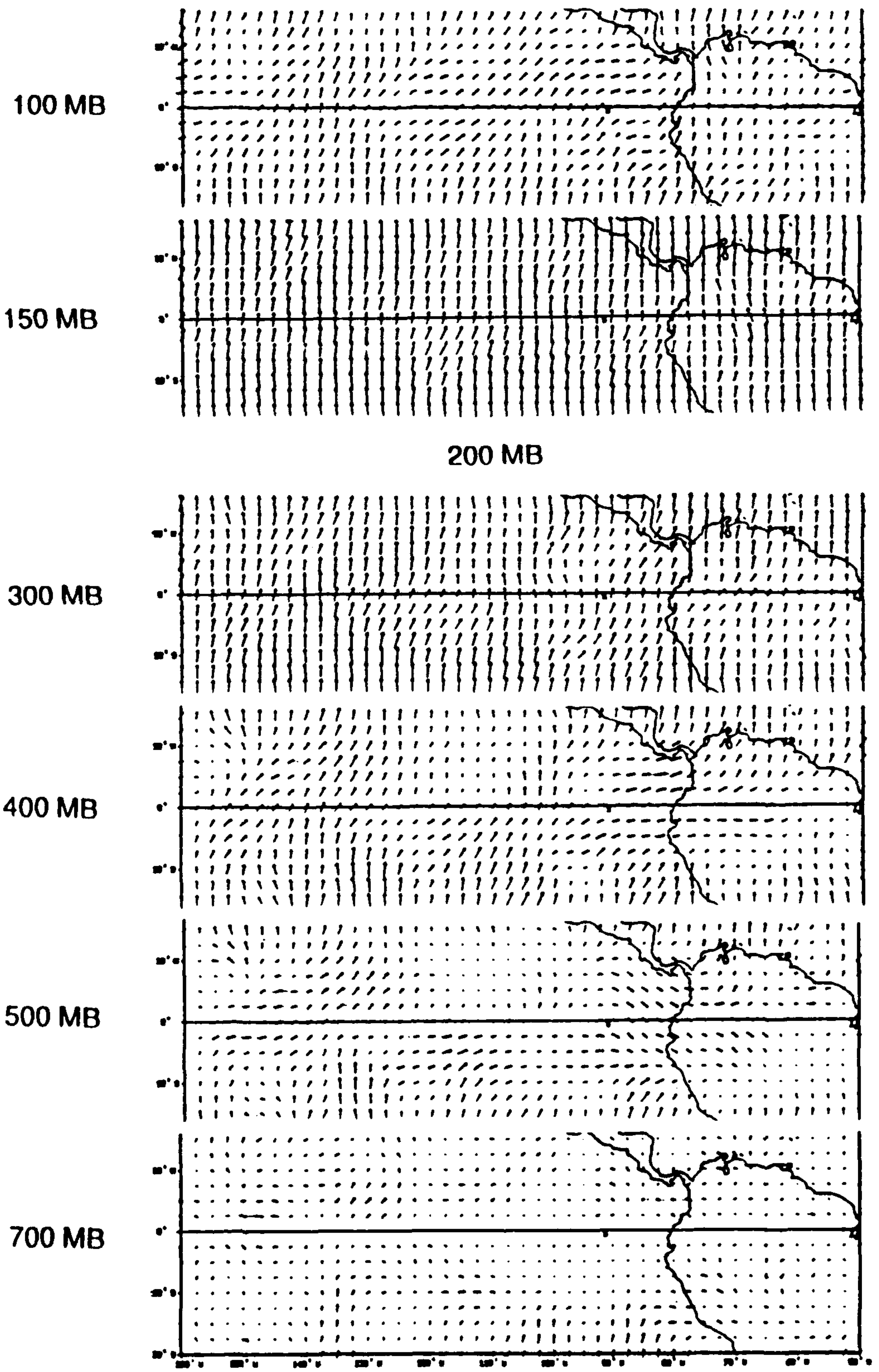

Figure 16c: Interlevel v200 comparison graph for 1991

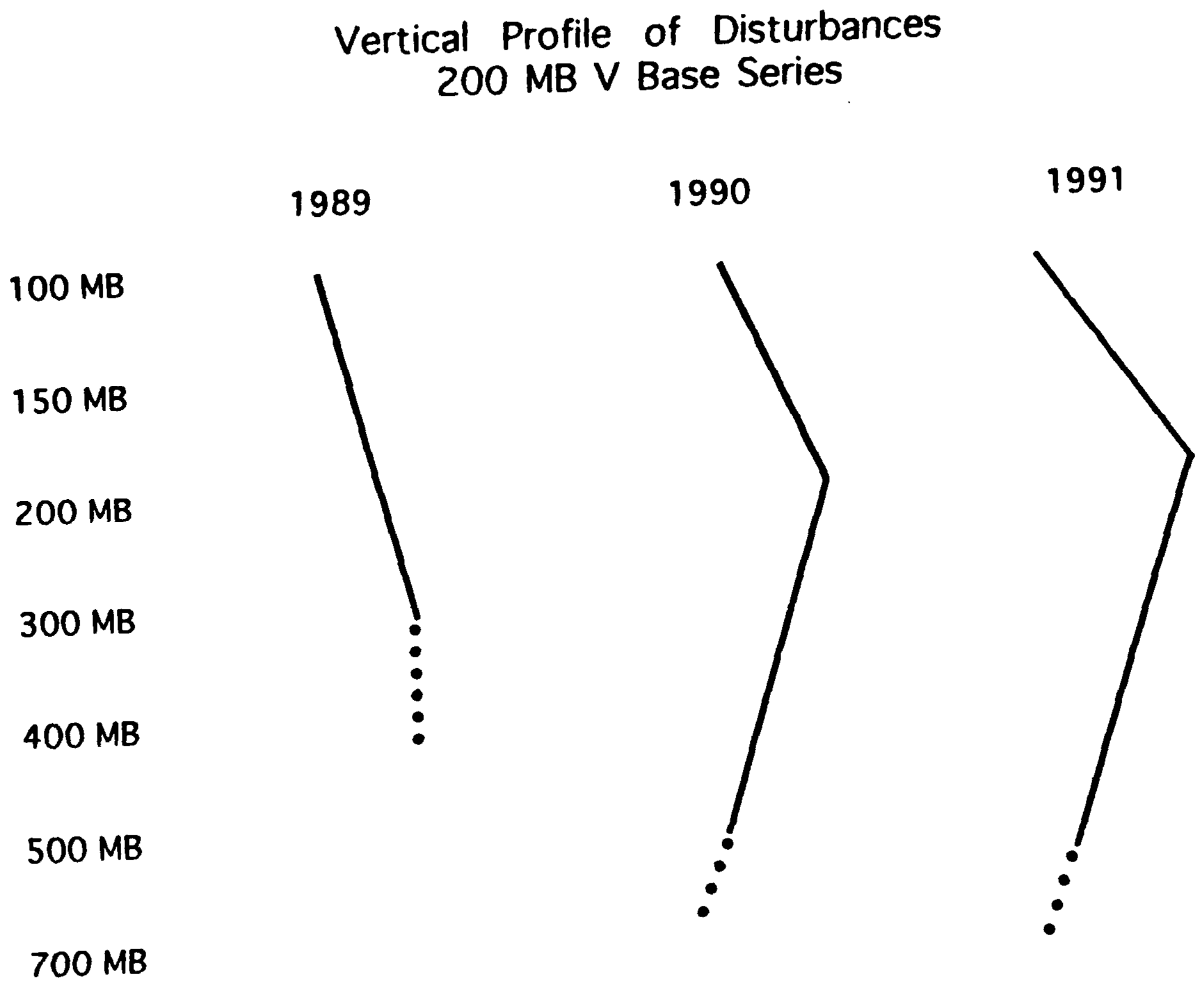

Figure 17: v200 profiles of vertical tilt
(uncertain levels dotted)

signals strong enough to provide significant coherences down to 500 hPa. The 1991 results show the strongest tilt and the highest coherence values. In all cases there are large regional differences.

B. LOWER TROPOSPHERIC VERTICAL STRUCTURE

The lower tropospheric vertical structure is determined from the cross spectra with v at 850 hPa as the base series. Figure 18 shows the coherence and phase vectors between v850 and v at 500 hPa, 700 hPa, 925 hPa and 1000 hPa for the three years. In general, all three years show a significant eastward tilt with height in the equatorial zone from 1000 hPa to 700 hPa, and continue to 500 hPa although with markedly reduced coherence. The total phase shift between 1000-700 hPa averages around 30°, with 1991 showing a slightly more prominent tilt of ≥ 45°. It may be noteworthy that over equatorial South America the tilt is westward with height between 850-700 hPa for all three summers. Outside of the equatorial zone, the tilt in the lower troposphere is generally westward with height south of 10°S but near barotropic (no tilt) north of 10°N. The latter feature agrees with Liebmann and Hendon's (1990) observation using the ECWMF analyzed data. However, at 500 hPa in the northwestern corner of our domain (near Hawaii) the vertical tilt is eastward with height for all three years.

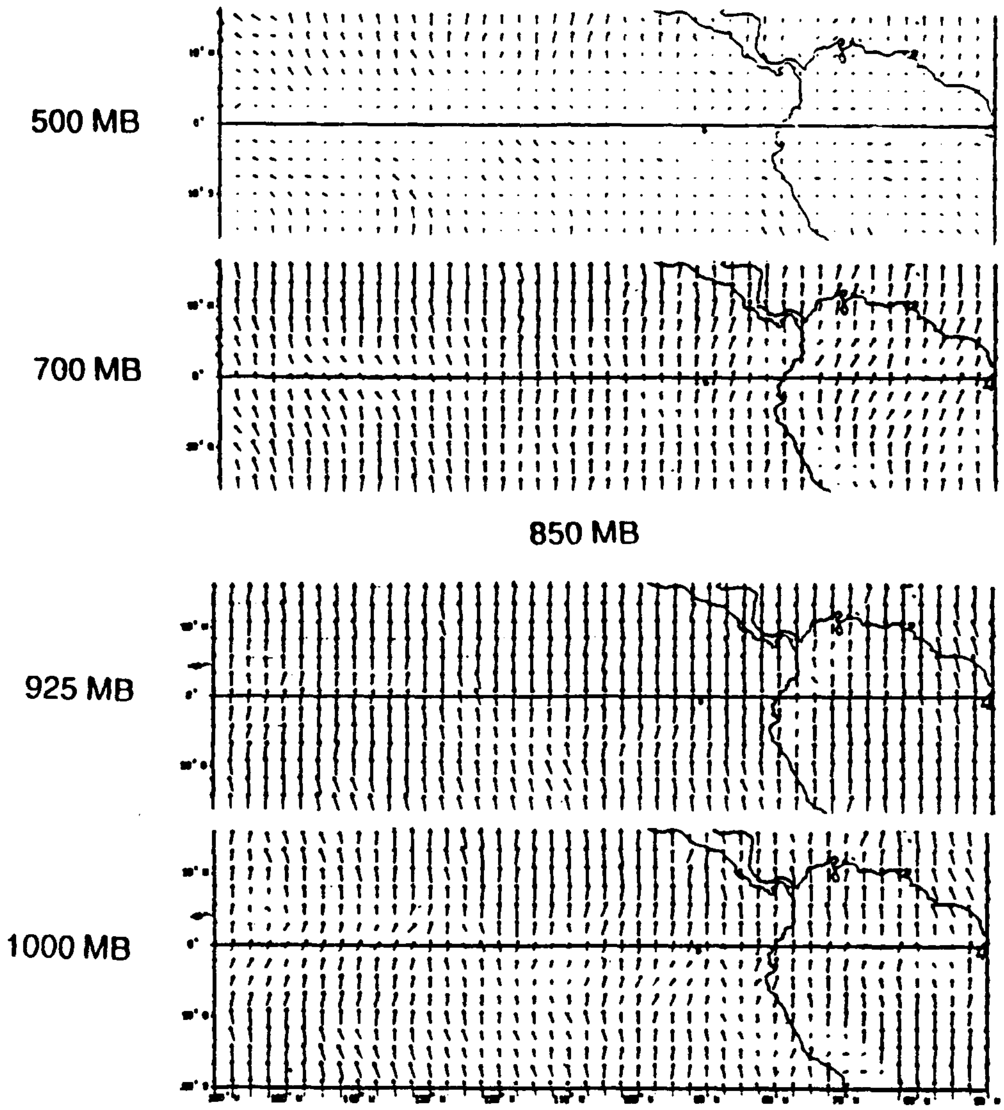

Figure 18a: Interlevel v850 comparison graph for 1989

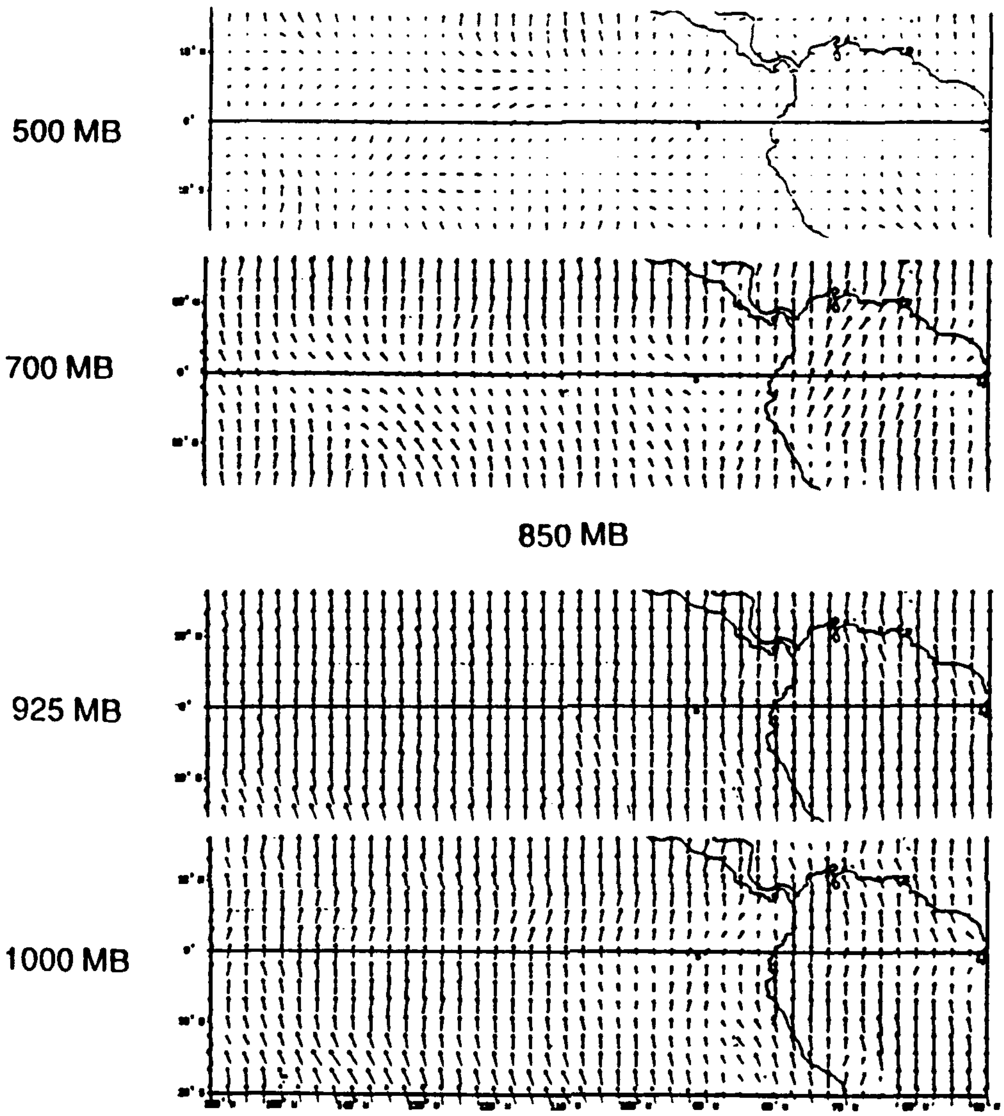

Figure 18b: Interlevel v850 comparison graph for 1990

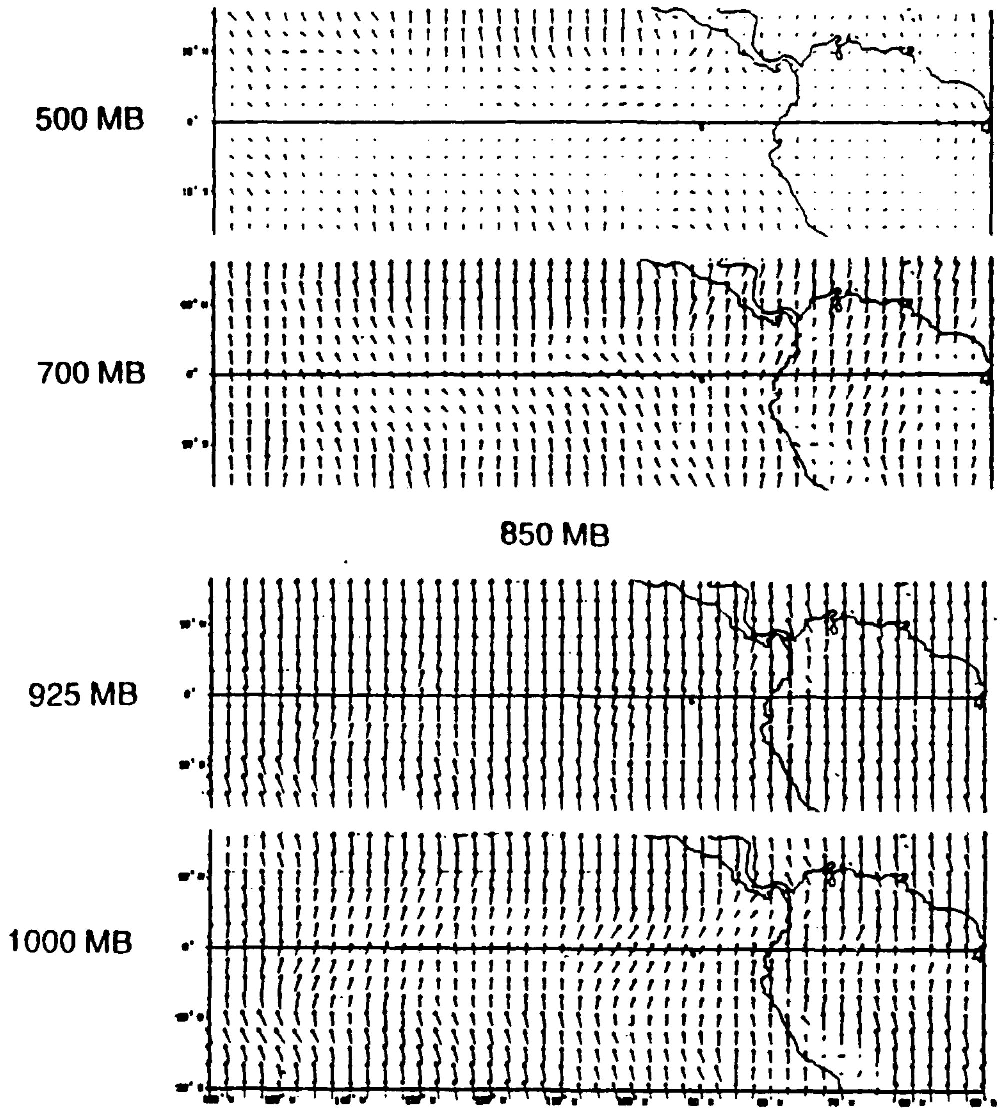

Figure 18c: Interlevel v850 comparison graph for 1991

Figure 19 is a schematic diagram of the vertical structure of the disturbances for the entire troposphere for the three years. It is a combination of the v850 cross-spectra with the v200 cross spectra results.

C. INTERANNUAL VARIATIONS OF TIME-MEAN ZONAL WIND

The different vertical tilt in the 300-200 hPa layer between 1989 (westward tilt with height) and 1990-1991 (eastward tilt with height) is the most prominent interannual variation in the vertical structure. Holton (1971) has conducted numerical simulations of the western and central Pacific easterly waves and suggested that the different vertical wave structure may be related to differences in the vertical shear of time-mean zonal wind. Figures 20-22 show the zonal wind, time-averaged within each of the three seasons, for 200 hPa, 400 hPa and 850 hPa, respectively.

At 200 hPa (Figure 20) the northern midlatitudes and most of the southern hemisphere are occupied by westerlies, with the equatorial region dominated by a zone of easterlies. The latter is a part of the northern summer tropical upper-tropospheric easterly jet that is centered near India (Krishnamurti and Surgi, 1987). For all three summers within the domain of study, the easterlies have the widest width near 110°W, but the width and maximum speed vary considerably. The 1989 (Figure 20) easterlies are strongest and cover a latitudinal span that reaches to 18°N to the west

Figure 19: Total profiles of vertical tilt
(uncertain levels dotted)

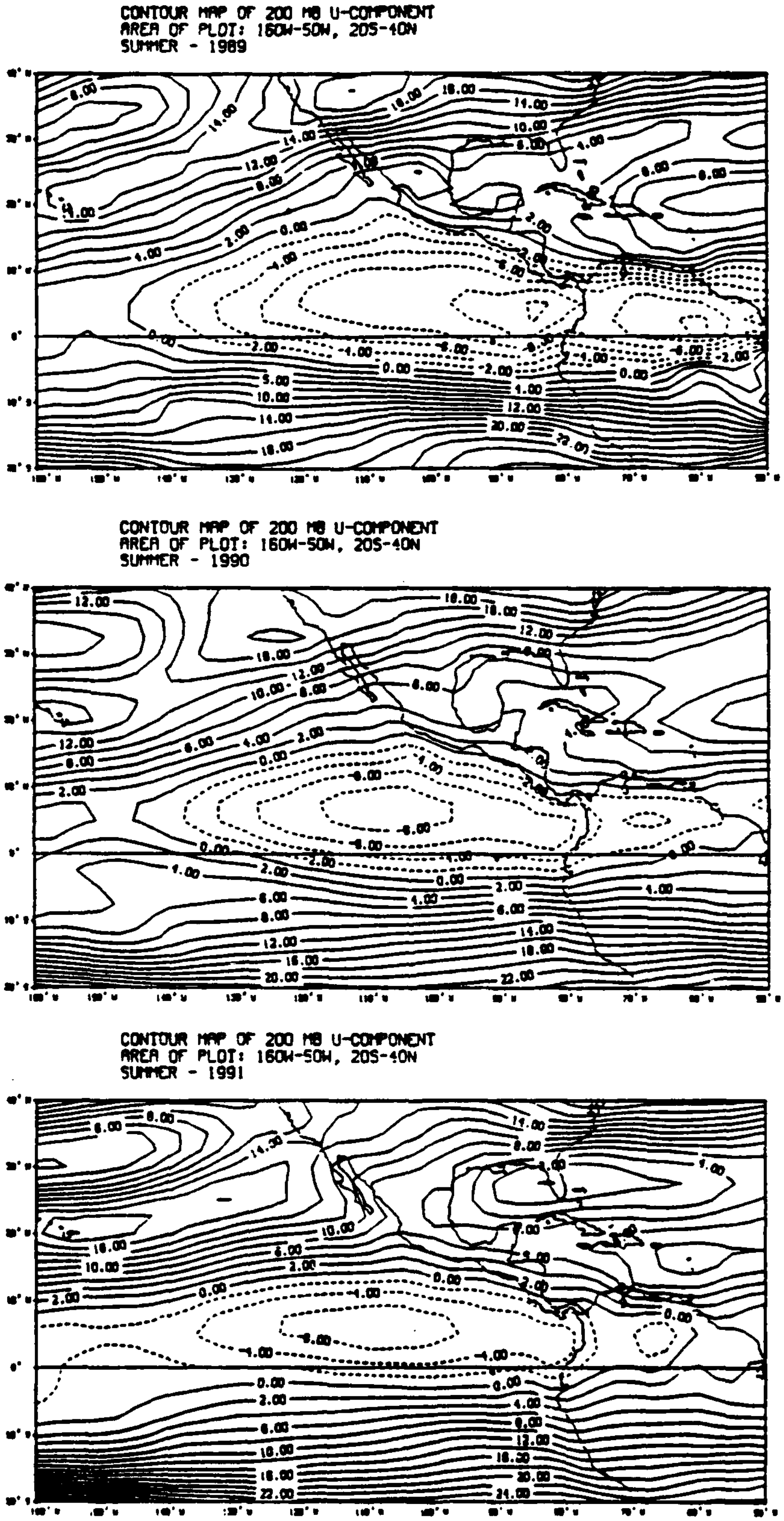

Figure 20: Contoured U200 (in meters/sec, easterlies dotted)

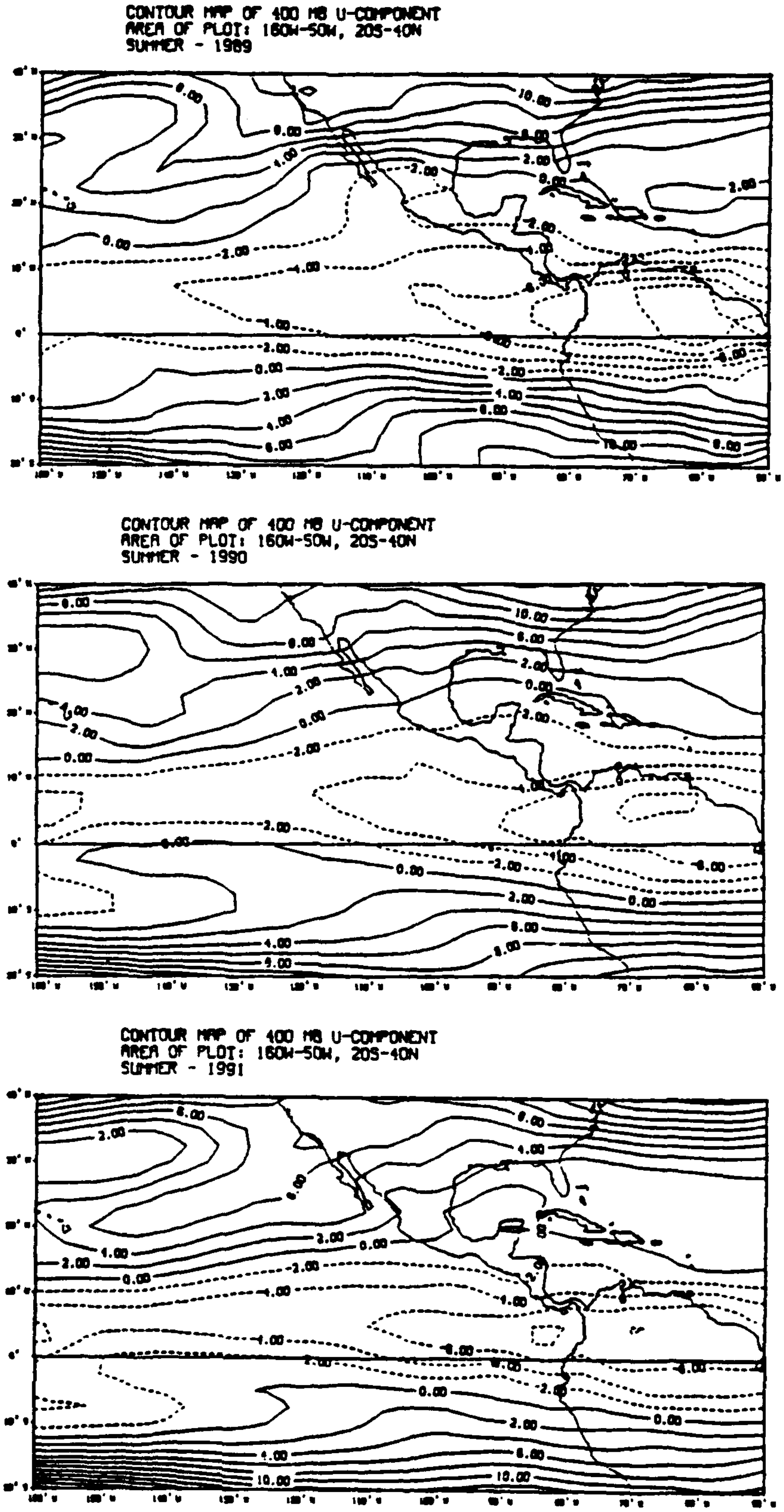

Figure 21: Contoured U400 (in meters/sec, easterlies dotted)

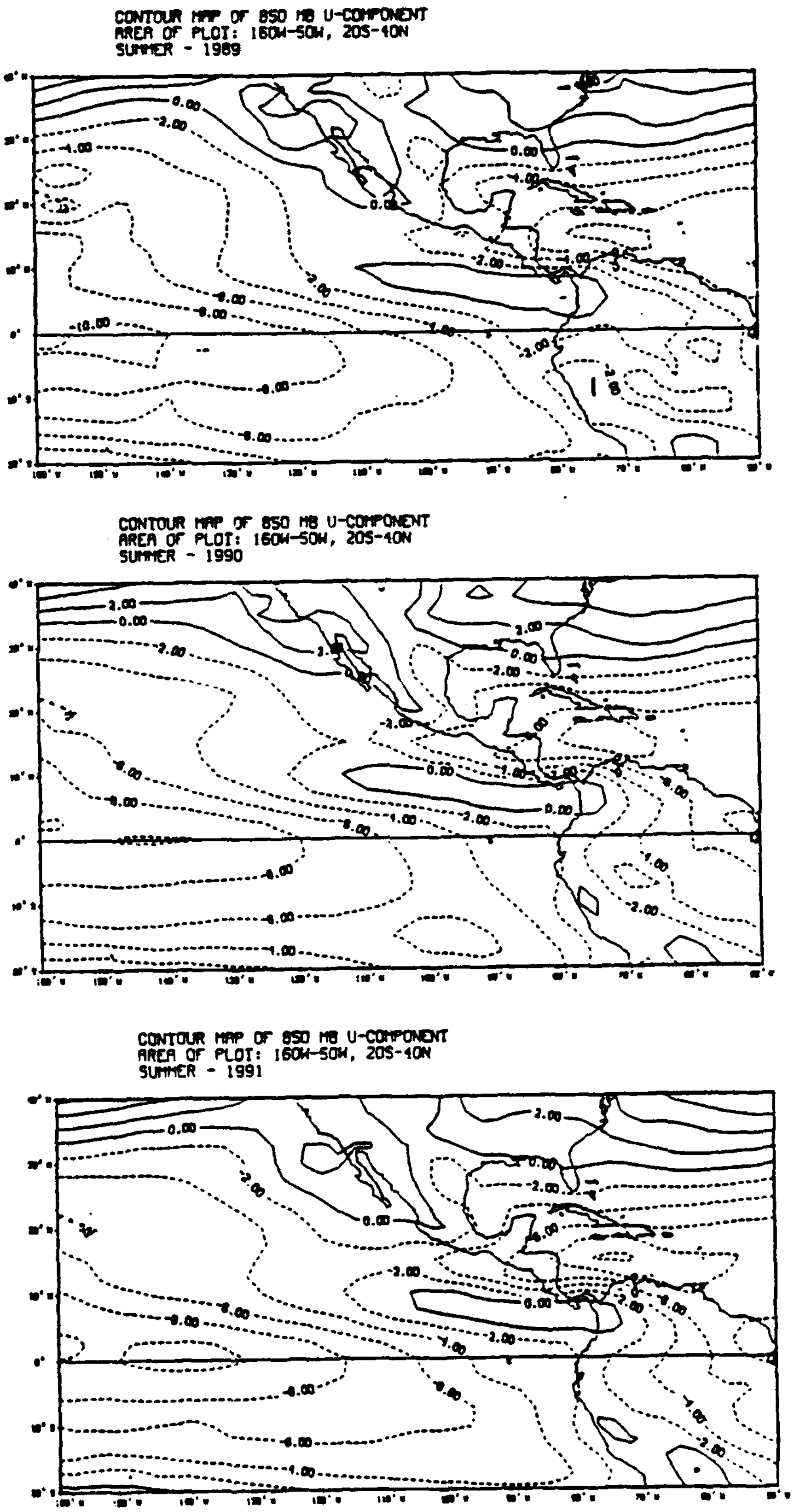

Figure 22: Contoured U850 (in meters/sec, easterlies dotted)

of Mexico. A large area in the equatorial eastern Pacific has easterlies of > 8 m/s, with the maximum of 12 m/s over and to the west of equatorial South America. In 1990 (Figure 20b) the easterlies cover a smaller region north of the equator and the maximum 8 m/s zone covers a much smaller area than 1989. In 1991 the maximum is less than 8 m/s and the total area occupied by easterlies is slightly smaller than 1990.

In contrast to 200 hPa, the seasonal mean zonal wind at 400 hPa (Figure 21) and 850 hPa (Figure 22) do not vary substantially from one year to another. So the greatest interannual variations in the vertical shear of mean zonal wind can be represented by the 200 hPa mean zonal wind in Figure 20. An independent source of data, the anomalous zonal mean wind (departure from a 1978-1987 ten-year average), can be found in the *Climate Diagnosis Bulletin* published by the Climate Analysis Center, NOAA. Figure 23 shows their August anomalous 200 hPa zonal mean winds for the three years. It is clear that the 1989 equatorial belt is dominated by anomalous easterlies. In Figure 23 there is a westerly anomaly along the equator near the western boundary of our domain in 1989. A similar but more extensive anomaly occurs in 1990, and in 1991 a westerly anomaly occupies most of the southern tropics. Thus the vertical shear of mean wind below 200 hPa is anomalously easterly in 1989, and somewhat anomalously westerly in 1991. These anomalous shears are in the same sense as the direction of the vertical tilt (westward with

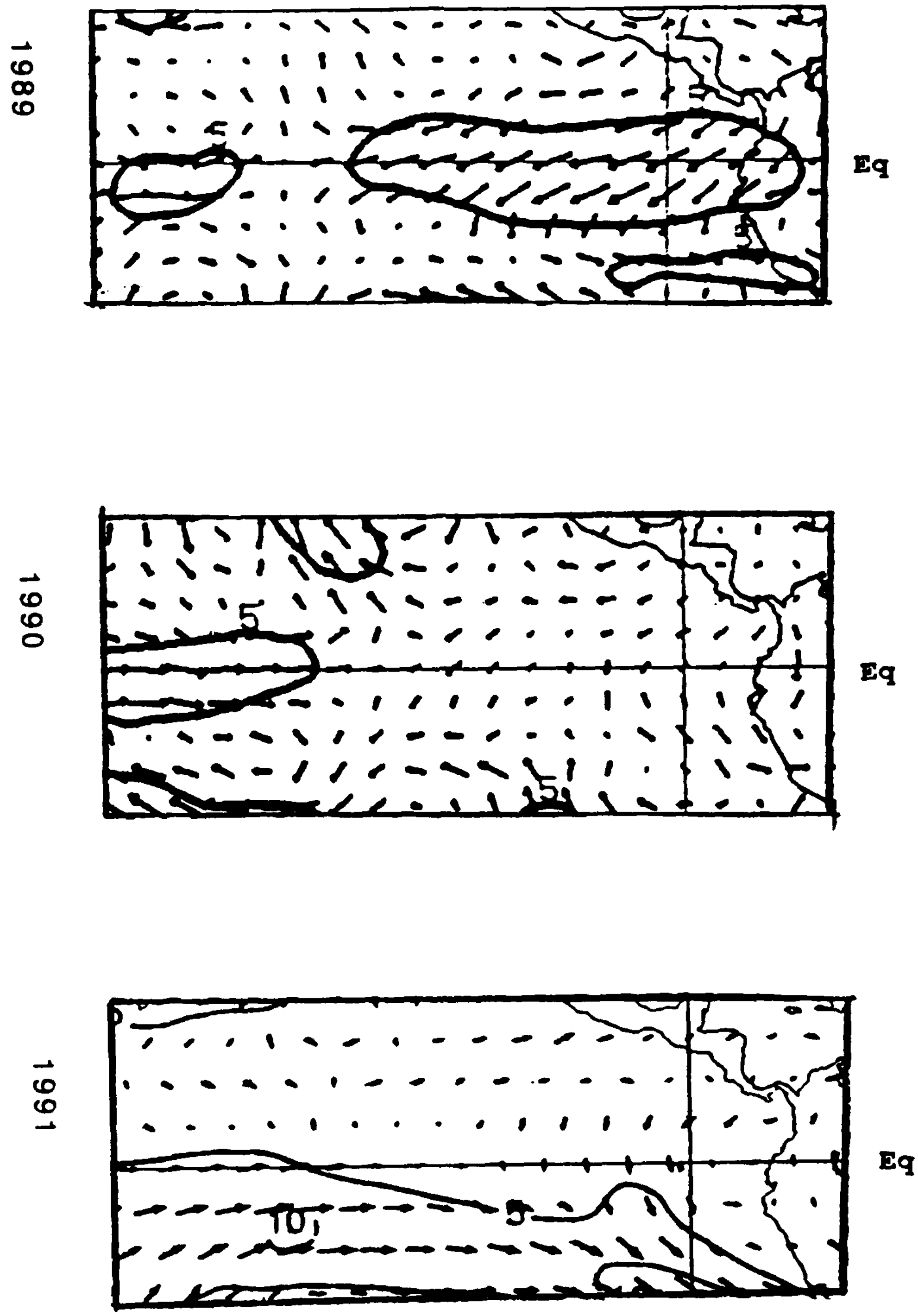

Figure 23: Anomalous 200 hPa winds from CAC *Climate Diagnosis Bulletin*

height in 1989 in the upper troposphere below 200 hPa, and eastward tilt in 1990 and stronger eastward tilt in 1991). These results are in agreement with Holton's (1971) numerical simulations.

On the other hand, the 200-150 hPa tilt is westward with height for all three years. Since the easterlies at 150 hPa (not shown) are weaker than at 200 hPa for all three years, the vertical tilt is in the opposite sense of the vertical shear. The vertical structure suggests that these are equatorial waves whose vertical structure is similar to internal gravity waves. For such waves, the vertical energy propagation opposes phase propagation, and the vertical tilts imply that the wave energy propagates upward and downward away from the 200 hPa level in 1990-1991, and from the 200-300 hPa levels in 1989. The comparison of the vertical tilts and the vertical shear of mean zonal wind suggests that the vertical shear affects the direction of energy propagation only at the levels immediately below 200 hPa. This is probably because the waves are excited in a layer whose top is at 200 hPa. Below 200 hPa, the vertical structure can change due to changing mean wind shear, so energy can propagate from 200 hPa downward or from 300 hPa downward. Above 200 hPa there is no energy source and energy can only propagate upward regardless of the vertical shear.

VI. DYNAMIC AND THERMODYNAMIC STRUCTURE: INTER-PARAMETER CROSS-SPECTRA

To study the complete structure of the disturbances, we performed cross spectra between various field parameters, usually using v200 and v850 as the base series.

A. THE STRUCTURE OF MERIDIONAL WIND VS ZONAL WIND COMPONENTS

Figure 24 shows the cross spectra between v at 15°N and u at all latitudinal points at 850 hPa. In the northern tropics an opposite phase vector with significant coherence can be seen over most of the domain. The phase vectors pointing westward (v leads u by a quarter cycle) near 20°N and those pointing eastward (v lags u by a quarter cycle) near 10°N combine to form a quasi-geostrophic u-v circulation relationship that resembles Rossby waves centered between 10°N and 20°N. Thus at 850 hPa the 3000-4000 km wavelength waves are centered near 15°N and resemble equatorial Rossby waves. Furthermore, the v and u phase difference at 15°N is in general less than 90°, suggesting an in-phase relationship which indicates a northeast-southwest tilt, consistent with the results inferred from the inter-y v cross spectra discussed earlier.

In the southern tropics, the coherence squares are generally much smaller. The incomplete structure based on

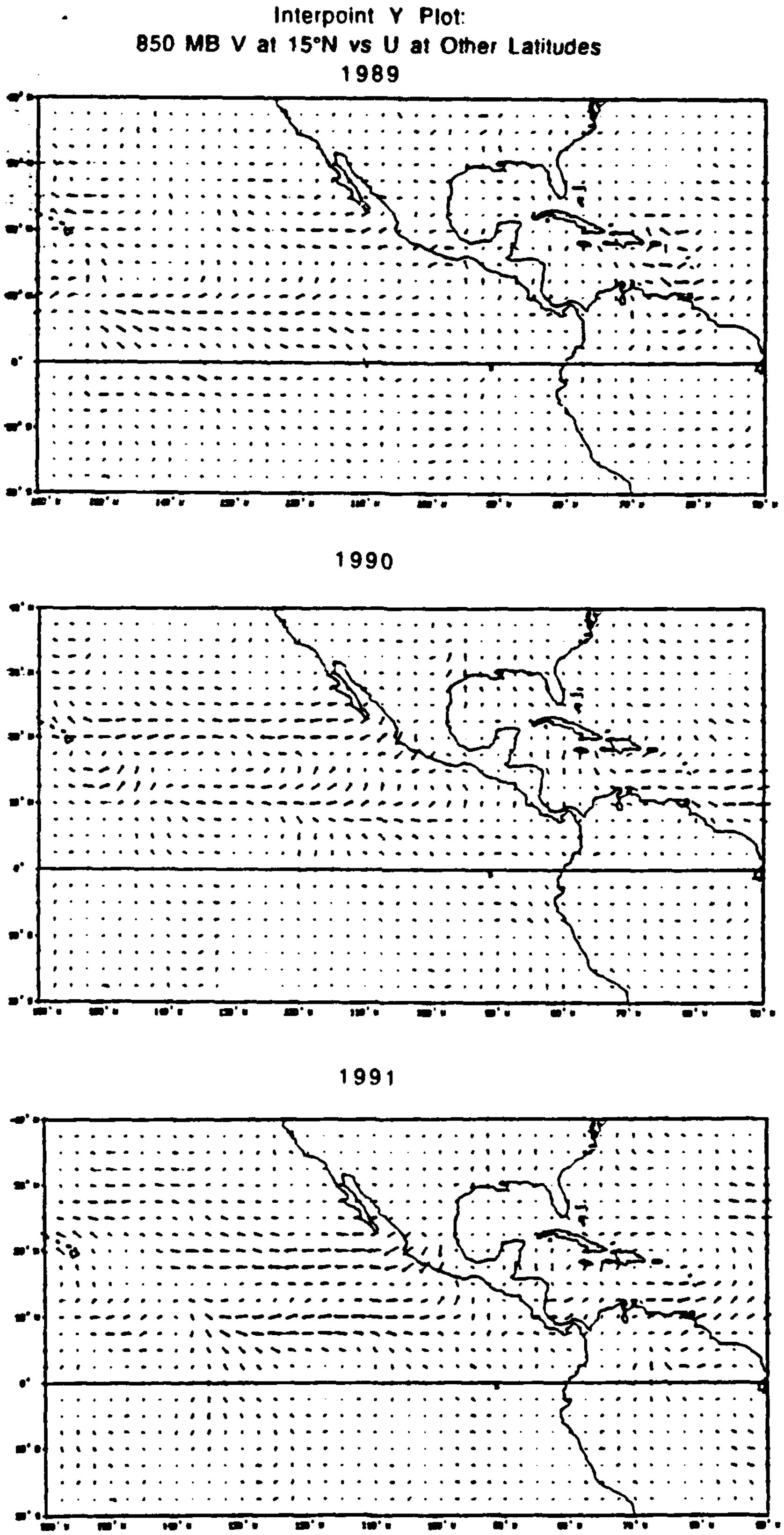

Figure 24a,b,c: Interpoint-y for v850 at 15°N vs U850 at other lats.

scattered points with marginally significant coherence does not appear to indicate a Rossby-type mode.

Figure 25 is the cross spectra between v at 15°N and u at other latitudes for the 200 hPa level. The opposing quarter-cycle phase vectors that are predominant in Figure 24 can still be seen but only in part of the northern tropics, particularly south and west of central America. In other areas the coherence is substantially lower. Thus the Rossby mode waves centered around 15°N are less organized in the upper troposphere than in the lower troposphere.

B. THE GEOPOTENTIAL HEIGHT STRUCTURE

Figures 26 and 27 show the cross-spectra between v, the base series, and the geopotential height (Ø) at 850 hPa and 200 hPa, respectively, for the three years. At both levels the phase vectors in general point westward in the northern tropics, where the coherence is large. This relationship indicates that v leads Ø in the east-to-west propagation disturbances, which is consistent with a Rossby (quasi-geostrophic) structure. At 200 hPa (Figure 27) the vectors point eastward in the northern midlatitudes, as would be expected with eastward propagating Rossby-type disturbances. Also at the upper level the strongest coherence occurs in 1991, again indicating that this is the most active year. Figure 27 also shows that in 1991 the v-Ø relationship has a particular feature that is not obvious in other years. The

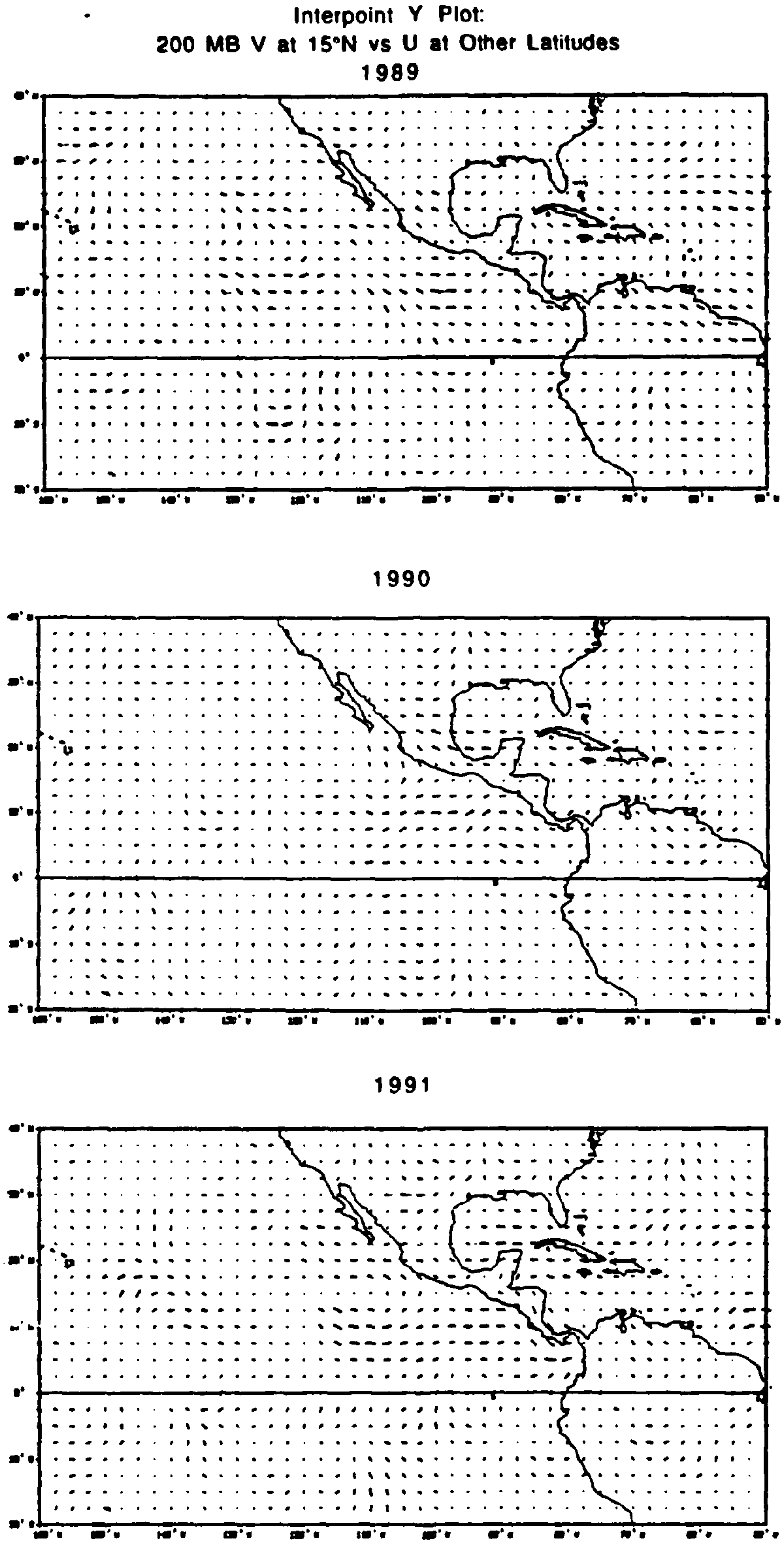

Figure 25a,b,c: Interpoint-y for v200 at 15°N vs U200 at other lats.

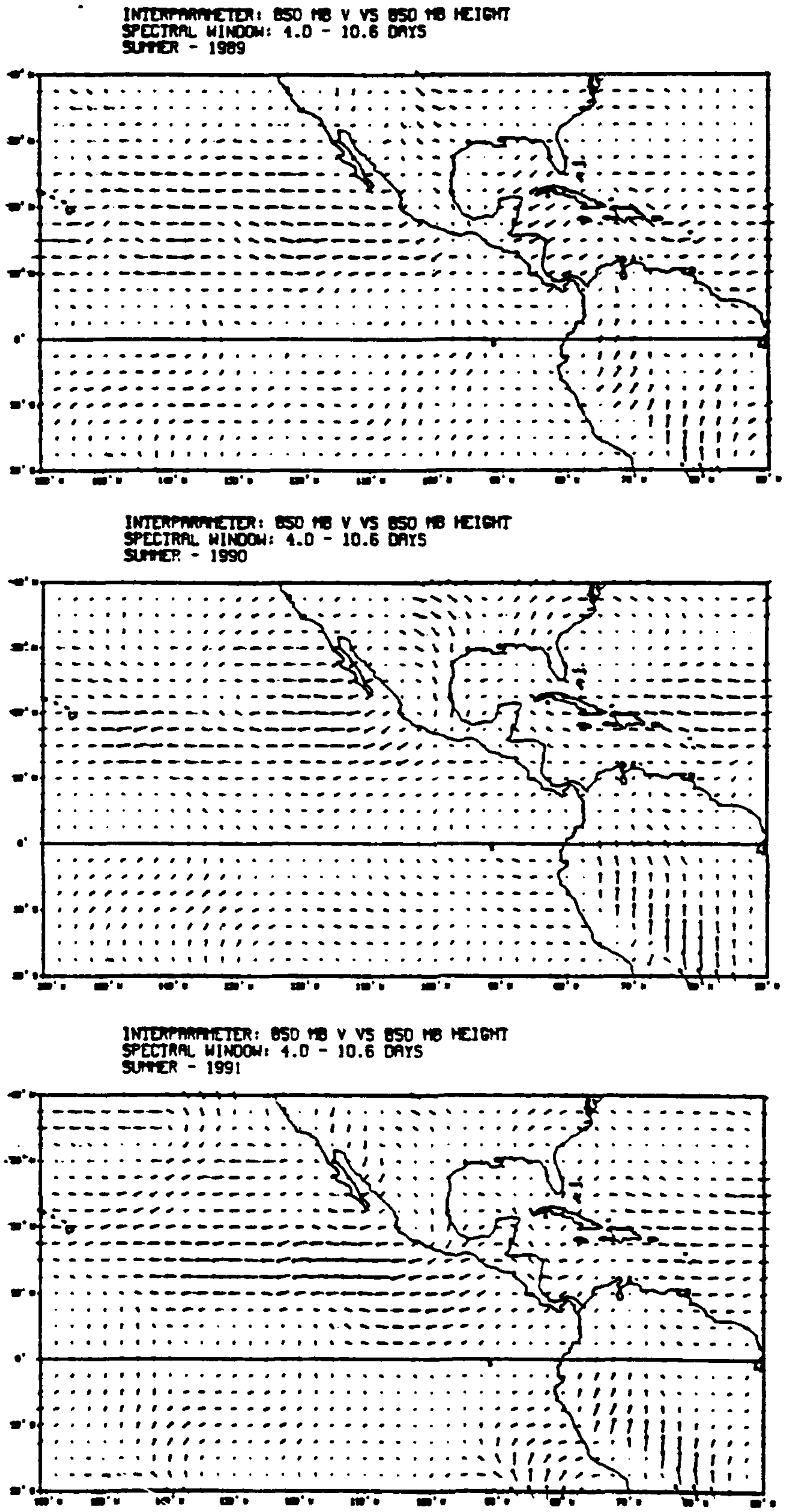

Figure 26a,b,c: Interparameter v850 vs Ø850 for 1989, 1990, 1991

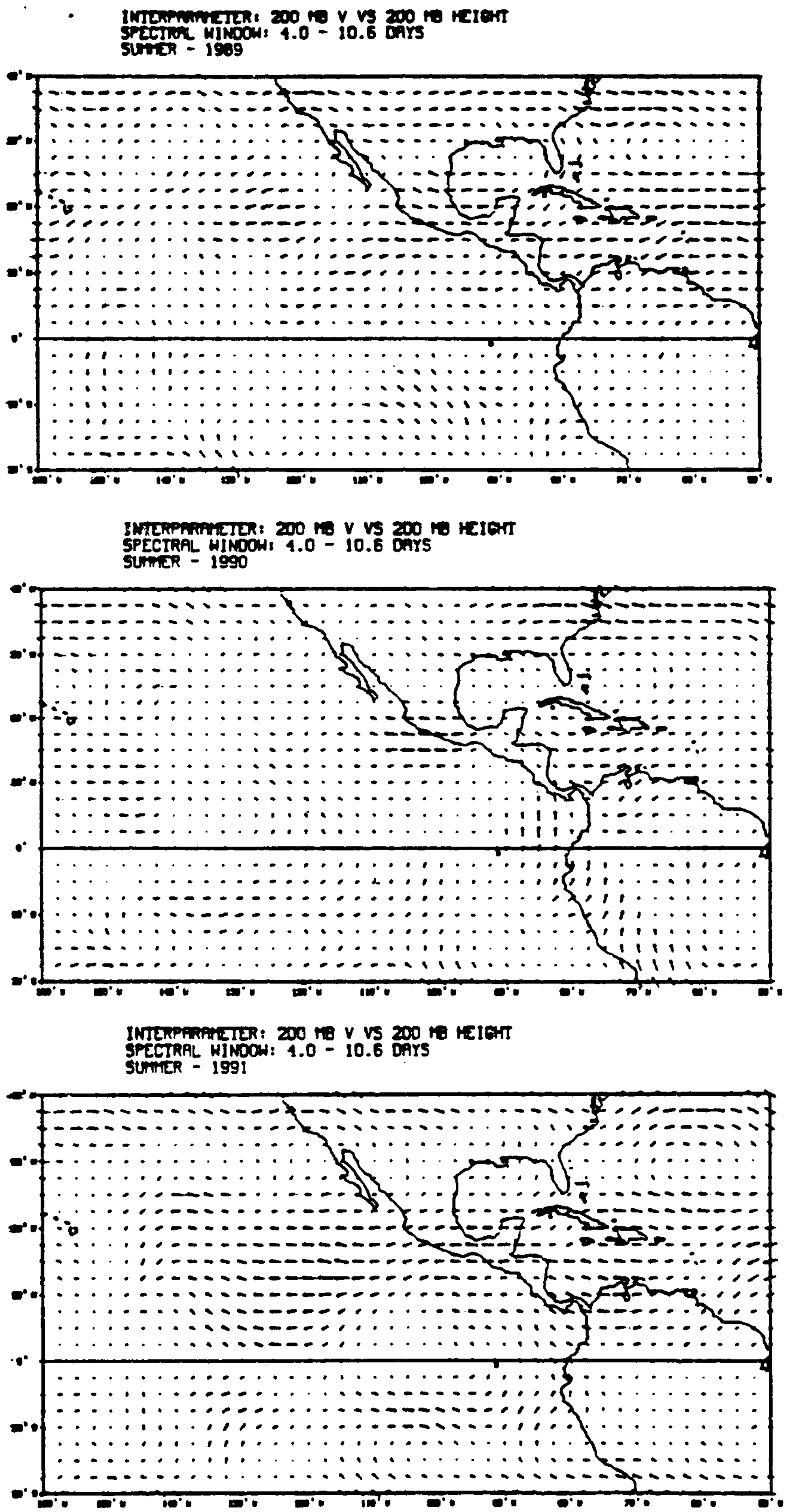

Figure 27a,b,c: Interparameter v200 vs Ø200 for 1989, 1990, 1991

direction of the phase vector fluctuates southward and northward over large zonal spans. If we focus on the 115°W-140°W sector, the vectors on the east side (115°W) point southward, indicating that v leads Ø by more than a quarter cycle. But on the west side (135°W), the vectors point northward, indicating that v leads Ø by less than a quarter cycle. A possible explanation for this shift in the v-Ø phase difference, assuming both propagate westward with the same periodicity of 4-10 days, is that Ø moves faster than v over this longitudinal span, or that Ø has a longer wavelength. The same v-Ø structure can be seen over the tropical north Atlantic and the Caribbean Sea. The region between Central America and 140°W seems to indicate a reversed v-Ø relationship, but the small coherence squares rule this out.

The differential propagation or different wavelength structures imply that there are meridional energy fluxes. Where v'Ø' >0 (phase vector pointing northward), the energy flux is northward, and vice versa. An examination of August 1991 satellite-derived precipitation charts (not shown) does not reveal a reason for the varying meridional energy fluxes in the three longitudes. So, we do not have an external source to explain the direction of energy fluxes.

In order to further investigate the apparently different scales of geopotential height, we examined the inter-x cross spectra of Ø in the same way as we did for v. Figure 28 shows the result at 200 hPa with Ø at 120°W as the base longitude.

During 1989 and 1990, there is westward propagation north of 10°N. However, there is not enough information to define a wave because coherence falls off away from the base longitude, and phase turning is only visible near the base longitude. During 1991 the wave structure is more clearly defined by the phase reversal between 100°W and 137.5°W, indicating a westward propagating wave with a wavelength of about 8000 km. This may explain the v-Ø relationship in this region, with a somewhat shorter wavelength (5600 km) for v and a longer wavelength (8000 km) for Ø.

At the equator, Ø is in-phase over all longitudes during 1989 and 1990, suggesting a zonally-symmetric (wavenumber zero) structure, but in 1991 a wavenumber one tendency to the west of the base longitude is indicated. Immediately south of the equator the wavenumber one structure is evident over a broad zonal span. This may be related to the wavenumber one pressure wave in the tropics that has been observed by many investigators. (Wallace and Chang 1969; Madden and Stokes 1975).

Figure 29 shows the inter-x cross-spectra for Ø at 850 hPa. The patterns are somewhat similar to those at 200 hPa. Wavenumber one can be seen at 10°S and southward. Westward propagation patterns can be seen only at 10°N and northward. The equatorial belt shows a wavenumber zero structure.

The long zonal scales of the Ø disturbances are expected from tropical scale analysis. Short-wavelength Ø fluctuations

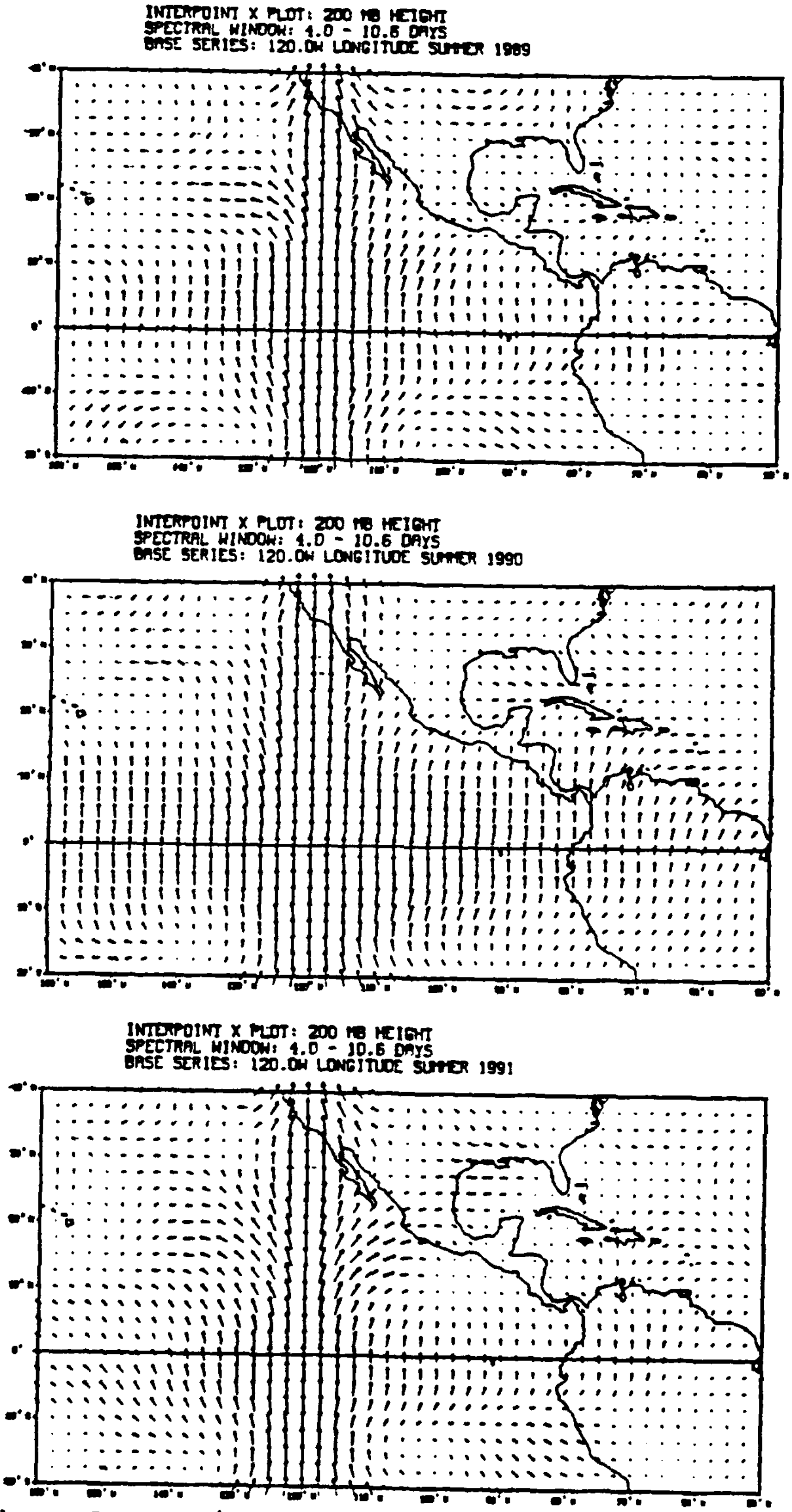

Figure 28a,b,c: Interpoint-x for Ø200 at 120°W in 1989, 1990, 1991

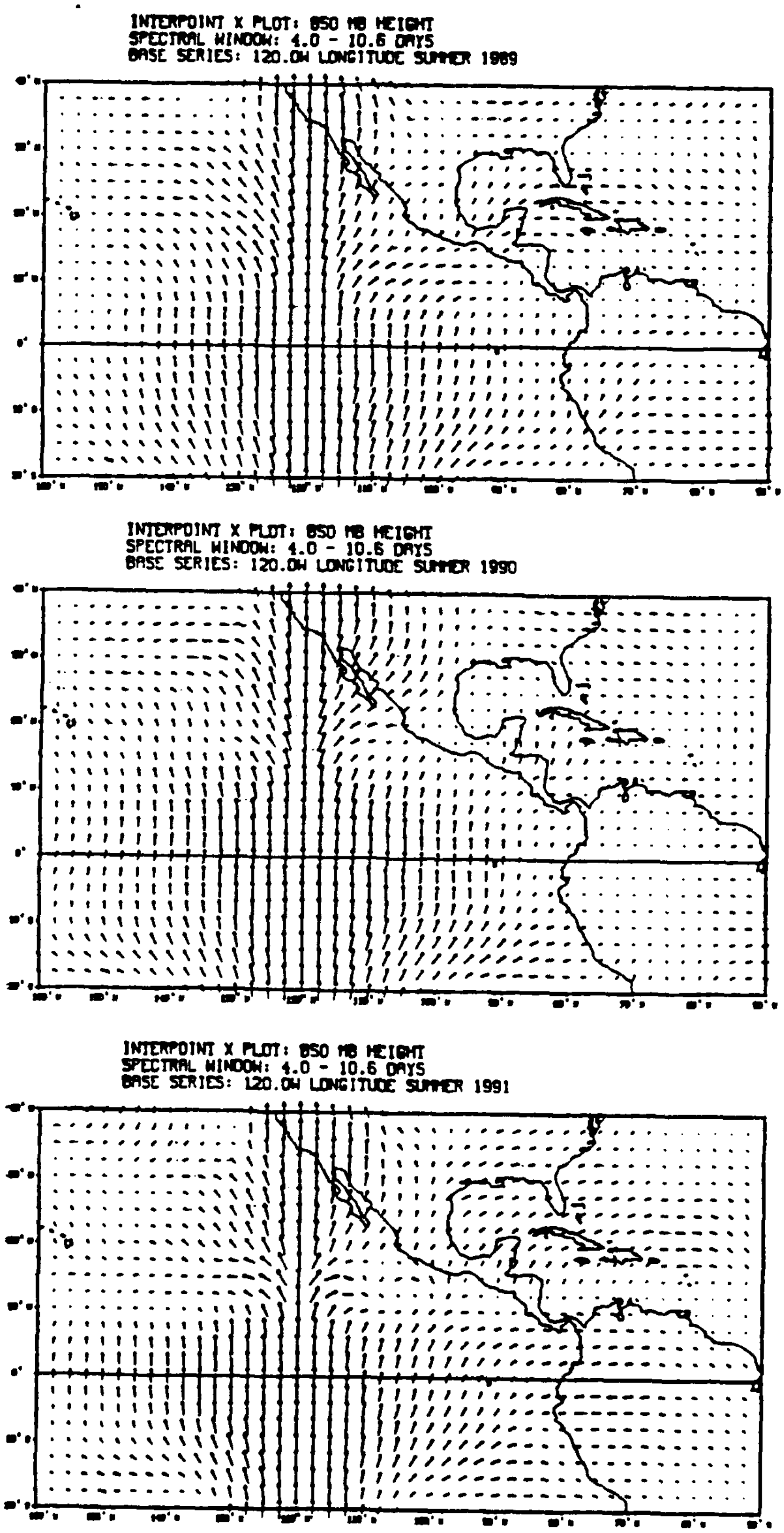

Figure 29a,b,c: Interpoint-x for Ø850 at 120°W in 1989, 1990, 1991

cannot have large amplitudes in order to keep wind fluctuations within bound. Very long scale Ø fluctuations can have relatively large fluctuations and still not be sufficient to produce detectable v fluctuations. However, it is possible that the 5600 km v waves interact with the 8000 km Ø waves locally as the scales are not very different. How the two disturbances coexist or interact is not clear at this time. Our results (Figure 27) seem to suggest that the two are synchronized in the eastern tropical Pacific and the Caribbean Sea. Whether this indicates that these are excitation areas for both waves, or that one interacts with another, should be a topic of future studies.

C. THE TEMPERATURE STRUCTURE

The thermal structure of the 4-10 day disturbances are determined from cross-spectra between v as the base series and temperature (T) at levels above and below. The use of different-level T is based on the hydrostatic consideration that the vertical structure as shown in Figure 19 should give maximum temperature fluctuations above and below the basic v-wave levels of 200 hPa and 850 hPa. Figures 30 and 31 show the results of v200-T300 and v200-T150, respectively, for 1989 and 1990. Unfortunately, the tropical temperature data for 1991 for the upper troposphere are missing from our archive. The coherence squares are generally small, apparently because the temperature fluctuations are small in

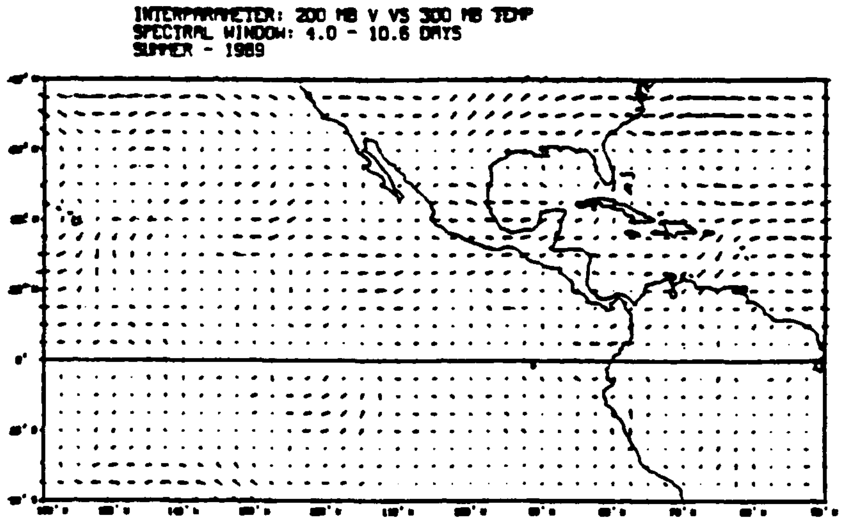

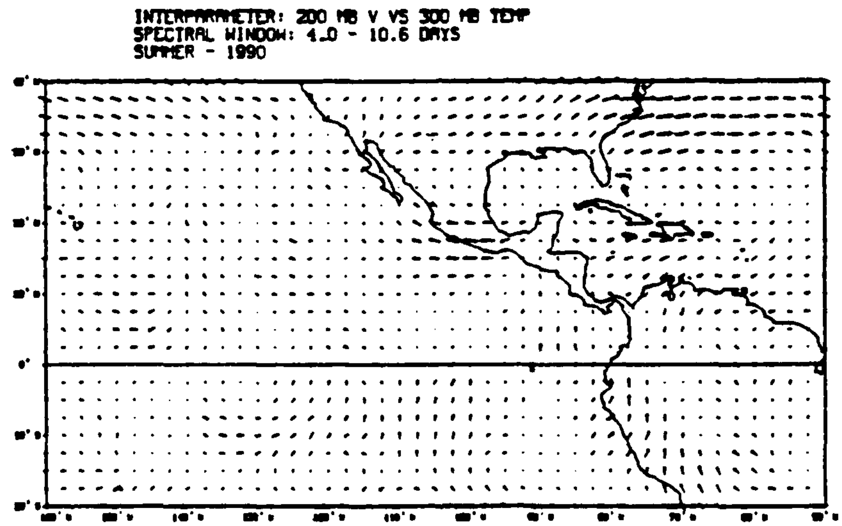

Figure 30a,b : Interparameter v200 vs T300 for 1989, 1990

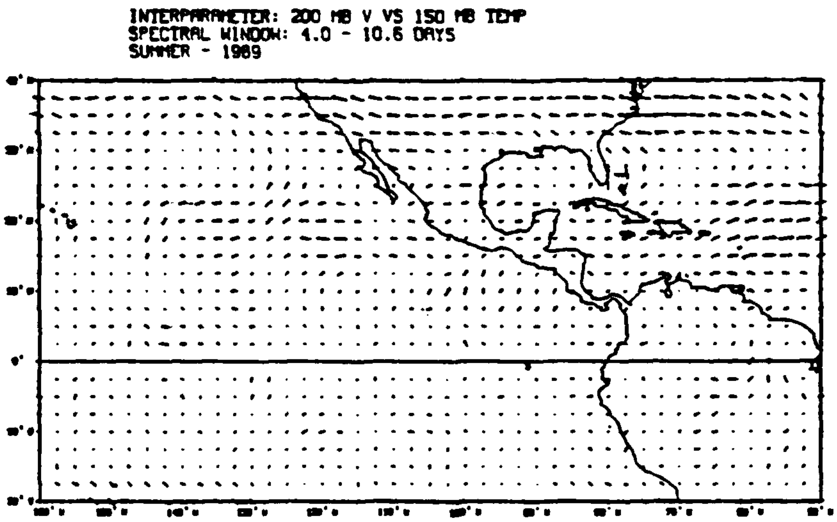

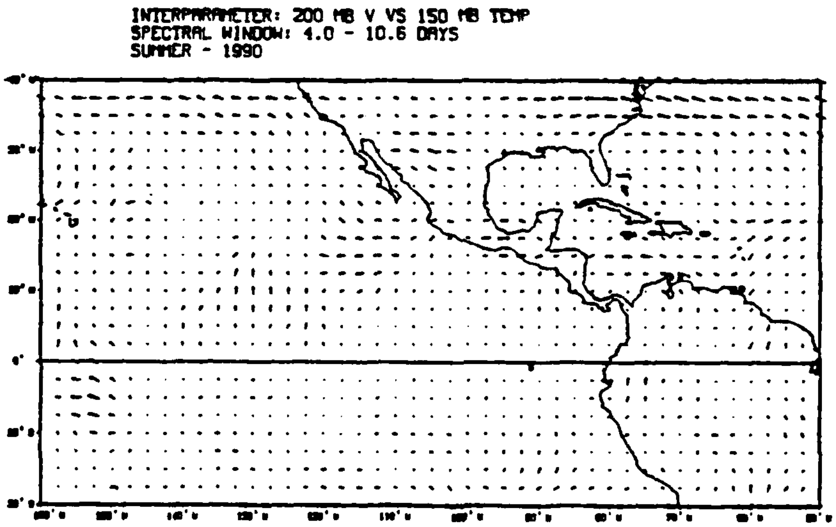

Figure 31a,b : Interparameter v200 vs T150 for 1989, 1990

the tropics. In both Figures 30 and 31 only a few places near 15°N have significant coherence squares. At this latitude the phase differences in Figure 30 indicate that v200 leads T300 by a quarter cycle. Thus, there is a cold core below the 200 hPa trough, and a warm core below the 200 hPa ridge, consistent with the structure expected from the hydrostatic balance. Figure 31 shows that at 15°N v200 lags T150 by a quarter cycle, or a warm core is above the 200 hPa trough, and a cold core is above the 200 hPa ridge, again consistent with the structure of hydrostatic balance.

The lower tropospheric thermal structure is shown in Figures 32 and 33, which show the cross spectra of v850-T925 and v850-T700, respectively, for all three years. Figure 32, shows that for all three years v850 leads T925 in the tropical northwest Atlantic and Caribbean region, and also near Hawaii. This phase relationship indicates that a cold core lies underneath the 850 hPa trough, which fits into the classical "waves in the easterlies" model proposed by Riehl (1948) for Caribbean Sea disturbances. For these waves, the maximum trough intensity is at 850 hPa. A striking exception that stands out clearly in the northern tropics occurs in 1991 (Figure 32), where an area of high coherence squares between 102.5°-122.5°W and 5°-15°N shows that v850 lags T925 by approximately a quarter cycle, indicating a warm core below the 850 hPa trough. Therefore in 1991 the maximum trough intensity over this area is near the surface rather

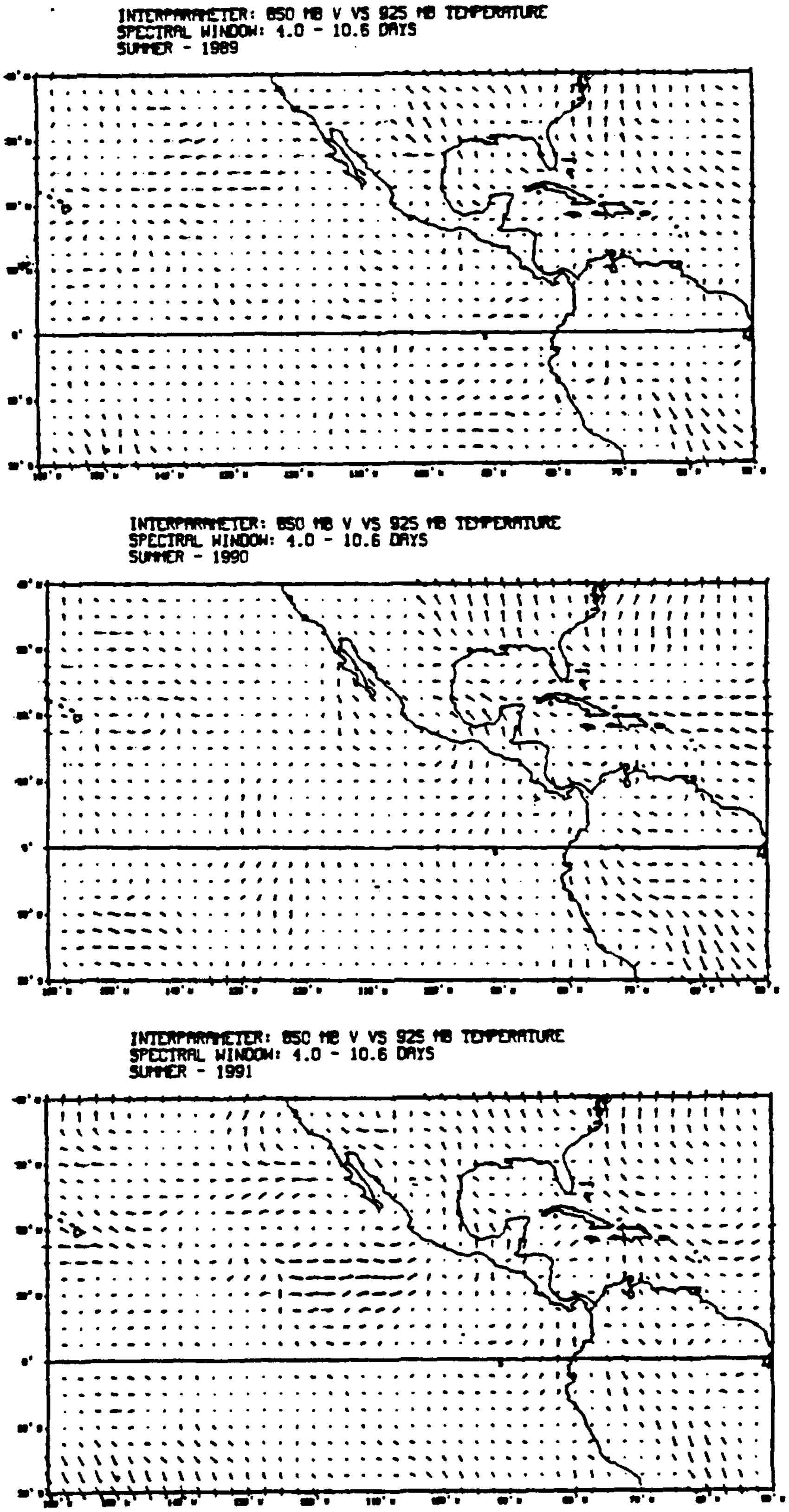

Figure 32a,b,c: Interparameter v850 vs T925 for 1989, 1990, 1991

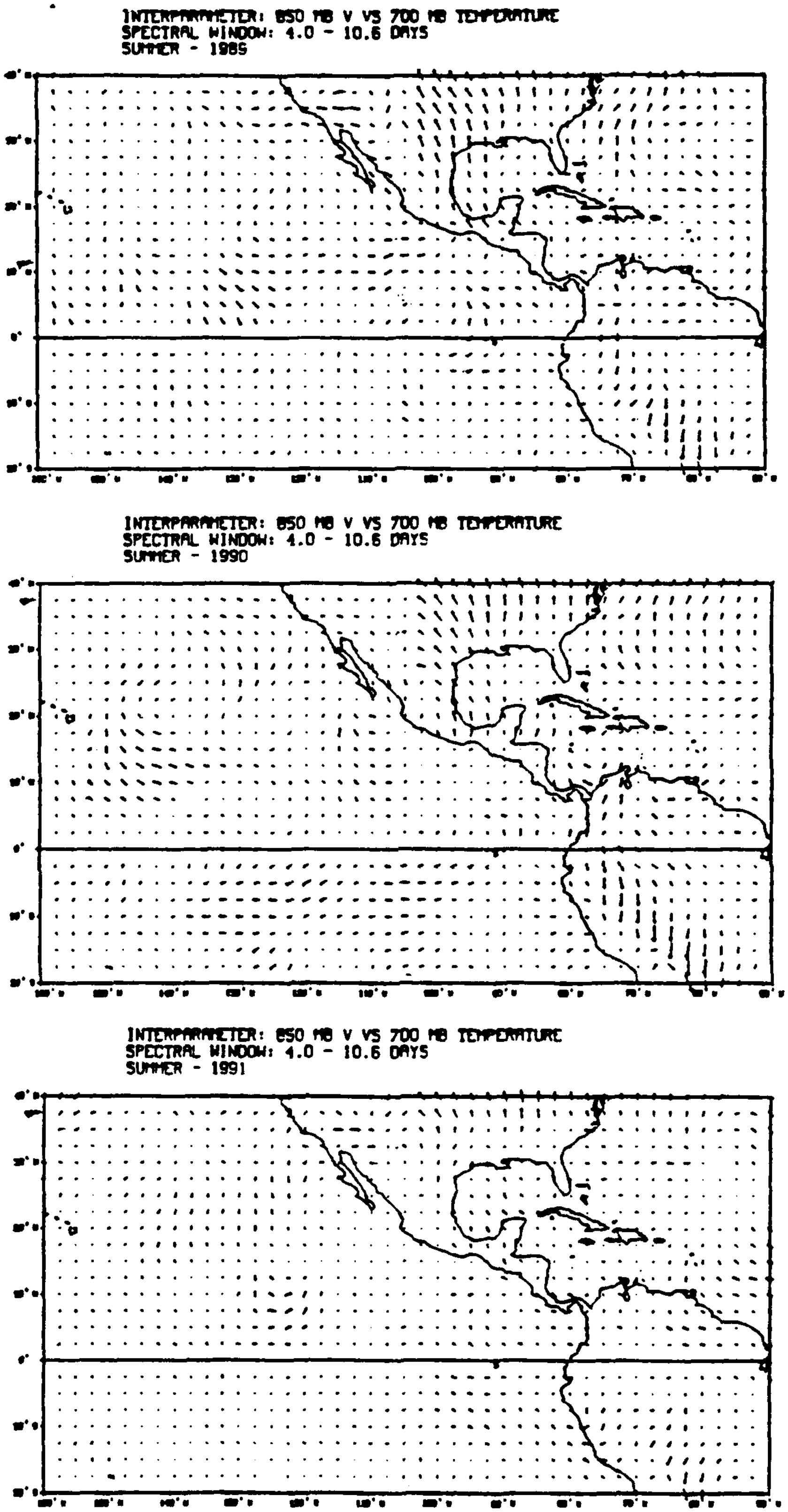

Figure 33a,b,c: Interparameter v850 vs T700 for 1989, 1990, 1991

than at 850 hPa. In the other two years the coherence squares in this area are very low. Since 1991 was an El Niño year, there is a possibility that the higher sea-surface temperature over the equatorial eastern Pacific may have affected the lower level thermal structure of the synoptic scale disturbances. More study will be needed to explain this "anomalous" low-level warm core in 1991.

Figure 32 also shows that the coherence between v850 and T925 is generally small along the equator, but reaches significant levels in the southwest and southeast (South American) parts of our domain. In these regions, v850 lags T925 by an average of 140°. This places the 925 hPa cold temperature center ahead of the 850 hPa trough axis in the southern hemisphere. This indicates that the low-level thermal structure there is slightly cold core with a poleward heat flux.

Figure 33 shows that in general the northern tropics v850 lags T700 wherever the coherence is significant. This is consistent with the hydrostatic relationship for a vertically eastward tilted wave. Comparison with the lower tropospheric inter-level cross spectra (Figure 18) confirms that this structure usually occurs over regions of eastward vertical tilt. Over South America, v850 and T700 become almost 180° out of phase, supporting the idea that this is a region of significant poleward heat flux in the lower troposphere.

In Figure 34 the cross spectra of v850-T500 are shown. Here the general structure, where coherence square is significant, resembles the v850-T700 result shown in Figure 33, with v lagging upper-level T in the northern tropics. The coherence squares for 1991 are remarkably high, again indicating stronger wave activities during this year, and larger temperature fluctuations at 500 hPa than at 700 hPa.

Based on the above results, a schematic diagram for the northern tropical region between the equator and 10-15°N is presented in Figure 35. This shows the vertical and thermal structure of the waves. This diagram resembles the easterly waves observed by Chang et al. (1970) for the central Pacific region. These waves had eastward tilts with height below 200 hPa and westward tilts above, a hydrostatic temperature structure, with equatorward heat flux in the lower troposphere, and poleward heat flux above 200 hPa. The vertical structure between 850-200 hPa is also similar to Liebmann and Hendon's along the date line, but the eastern Pacific waves in our diagram shows a stronger tilt. Liebmann and Hendon did not include levels above 200 hPa.

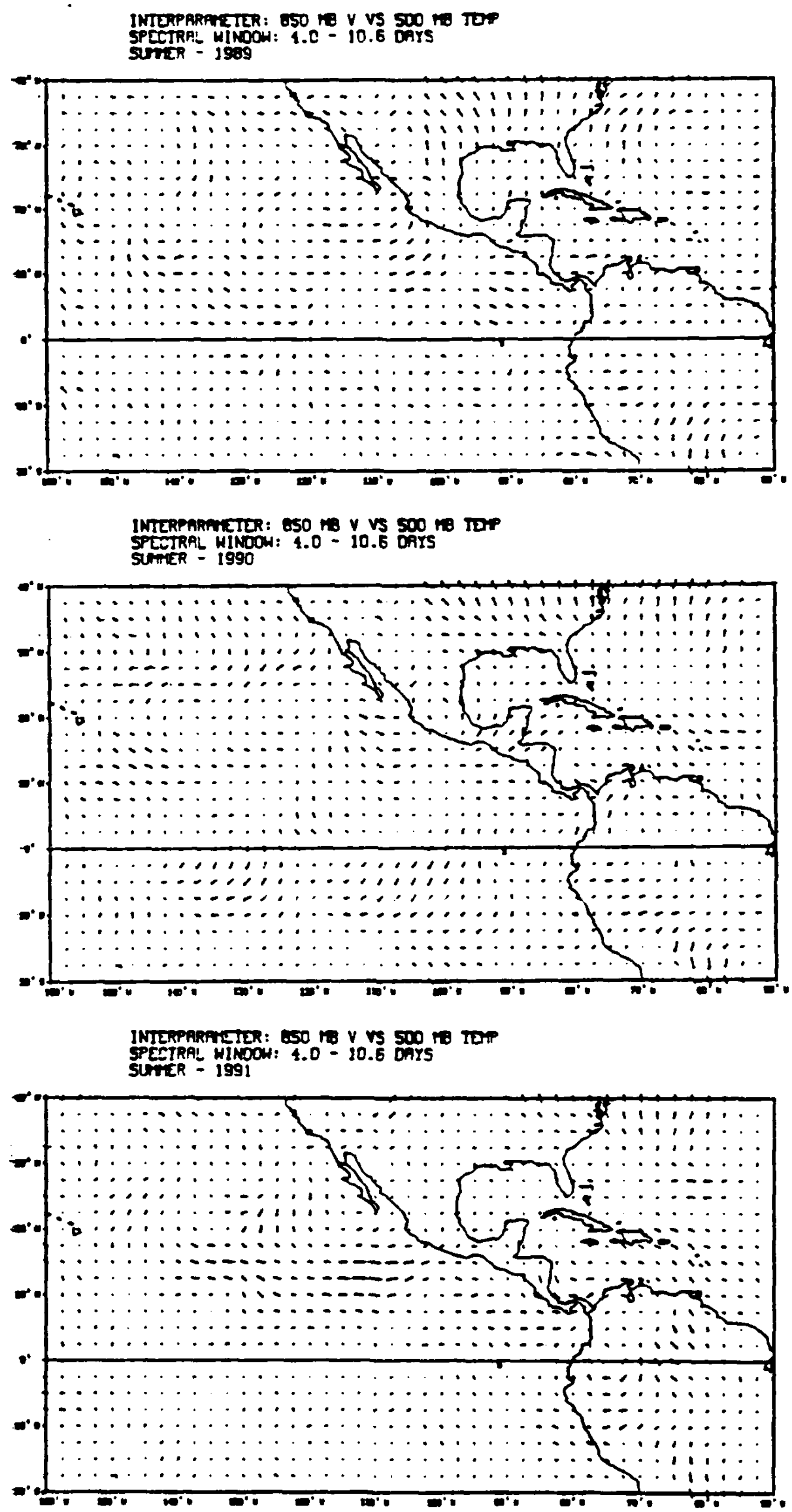

Figure 34a,b,c: Interparameter v850 vs T500 for 1989, 1990, 1991

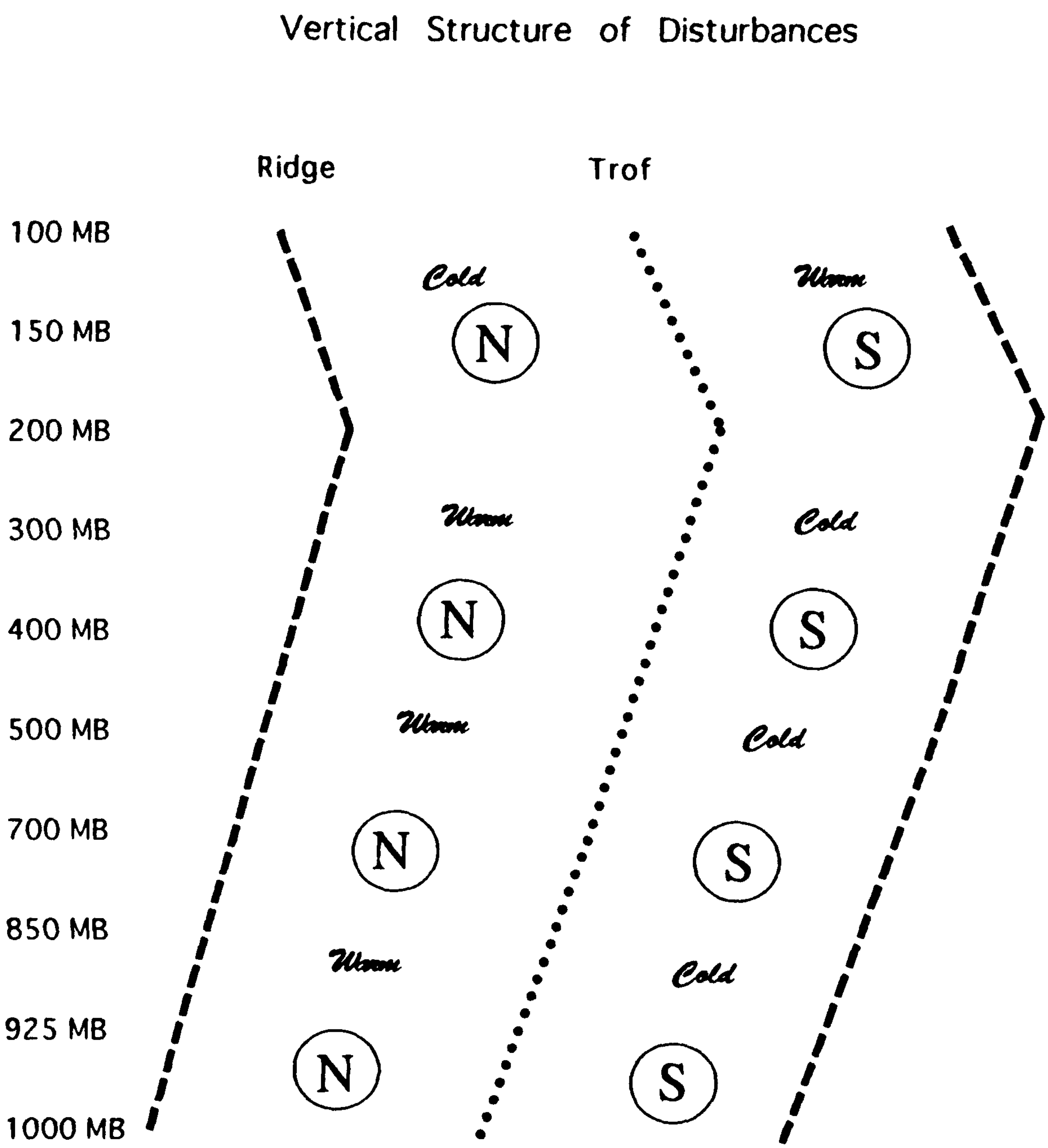

Figure 35: Vertical structure of winds and temperature

VII. SUMMARY AND CONCLUSION

We used the analyzed fields of the NOGAPS assimilated data over the tropical eastern Pacific to study the northern summer synoptic time-scale disturbances using spectral and cross-spectral analyses. The period of study is May-September 1989-1991, the three years when the latest version of the NOGAPS model was operational and data were available to us. The main conclusions are as follows:

1. There are significant variances in the meridional wind component in the 4-10 day range over the tropical eastern Pacific, both in the upper and lower troposphere.

2. The horizontal wavelength of the 4-10 day disturbances, based on meridional winds, is 3000-4000 km in both northern and southern tropics. The wavelength is 5000-6000 km or even longer in the immediate vicinity of the equator (between 10°N and 10°S).

3. The equatorial waves are weakest in 1989 and most prominent in 1991.

4. Along the equator the vertical tilt is eastward with height from the surface (1000 hPa) upward into the upper troposphere. In 1990 and 1991 this eastward tilt extends to 200 hPa and where the tilt becomes westward to the tropopause (100 hPa). In 1989 the eastward tilt extends to 400 hPa only, above which the tilt is westward with height. With some local

exceptions, north of 10°N the tilt is very slight throughout the troposphere. This is consistent with Liebmann and Hendon, who found a barotropic vertical structure in the northern tropics. South of 10°S the tilt in the upper troposphere is similar to the equatorial waves, but in the lower troposphere the tilt tends to be westward with height, suggesting a different type of disturbance.

5. The difference in the 400 hPa-200 hPa vertical tilt between 1989 and the other two years is in the same sense as the difference in the vertical mean zonal wind shear. In 1989 the 200 hPa equatorial easterlies are anomalously strong, so the mean flow shows an easterly shear vs. a westerly shear in 1990-1991, when the equatorial westerlies are anomalously strong. This "tilt in the direction of shear" is in agreement with the numerical simulations by Holton for western Pacific easterly waves.

6. The vertical tilt indicates that the waves developed in the upper troposphere, at about 200 hPa, during 1990-1991 and at about 200-300 hPa during 1989, and that they propagate energy upward to the tropopause and downward to the lower troposphere. This structure is similar to that found over the central Pacific in previous studies.

7. The v-u cross-spectra indicate that 15°N is a central latitude for the meridional wind fluctuations, with opposing u components to the north and south in a pattern consistent with a Rossby-type wave structure.

8. The v-Ø cross-spectra show a general gradient wind relationship except very near the equator. However, in 1991, the year of most organized wave activities, there is a consistent change of phase shift from east to west in the eastern Pacific, suggesting that the Ø waves have a somewhat faster phase speed (a longer zonal scale).

9. The v-u and v-Ø cross-spectra suggest that the 3000-4000 km waves in the northern tropics may be an equatorial Rossby wave. The coherences between these parameters for the equatorial 5000-6000 km waves are low. Based on the longer wavelength and the fact that prominent oscillations occur in the equatorial v component only, they appear to be mixed Rossby-gravity waves.

10. The wavelength determined by the Ø data shows an almost zonally symmetric geopotential height fluctuation along the equator for 1989-1990, and a westward propagating pattern in both hemispheres outside the equatorial zone. Only in 1991 can a Ø-wave pattern be clearly identified with a wavelength of near 8000 km.

11. The longer wave scale (wavenumber zero or one) that was detected in Ø is consistent with tropical scaling arguments. However, the relationship between the long Ø-fluctuations and the short v-waves is unclear, since the latter's signals in Ø are masked by the former. An interesting exception is 1991 when an 8000-km Ø wave was observed. It appears that there might be a synchronization of

the two waves in the eastern Pacific and in the western North Atlantic-Caribbean regions.

12. The temperature structure found for the northern tropics is consistent with the hydrostatic relationship, with cold air below the trough and warm core above. The vertical structure suggests that the temperature fluctuations have the same eastward vertical tilt as the v-waves below 200 hPa. Above 200 hPa a warm core occurs over the 200 hPa trough. So the meridional heat flux is equatorward above 200 hPa and poleward in the lower troposphere.

The vertical tilt might be affected by the way the near "single-level" satellite wind data are analyzed in the model, as there is no radiosonde data over the tropical eastern Pacific. A possible effect of this is that whenever there is a change of observed satellite wind at 200 hPa that is substantially different from the first guess (the six-hour model forecast), the incremental change in modifying the first guess will be largest at 200 hPa, and smaller at other levels (depending on a prescribed vertical influence function). Thus there may appear to be an energy source at 200 hPa level that propagates energy upward and downward. However, this effect would be important only if the satellite wind reports, averaged over a horizontal scale comparable to that of the horizontal wavelength, are consistently different from the area-average of the first-guess winds. The fact that the vertical structure is quite similar to that observed in

previous studies in the adjacent central Pacific, and that both structures are consistent with the Christmas Island radiosonde results (Yanai et al., 1968), indicates that the deduced vertical structure is probably not a mere artifact of the primarily single-level satellite winds.

Our study leaves many unanswered questions for which further study is needed. The different wavelengths deduced from the inter-x cross spectra for different latitudes, and for v and Ø, may be studied separately by zonal filtering. Similarly, the symmetric and anti-symmetric structures (with respect to the equator) can be separated. In this study we looked only over large areas and ignored detailed local variations of the vertical and horizontal structures. These may be examined by more detailed comparisons or correlation with the spatially-varying time mean flows. We noticed that there are some interannual variations between the three summers. Data for 1992 are now becoming available and can be included in future studies. Because of the somewhat scattered distribution of variances in the frequency domain, we averaged a rather broad spectral window between 4 and 10.6 days. It may be worthwhile to attempt to work with a more focused frequency window, particularly in the study of different wavelength signals from v and Ø. Finally, an independent data set, such as outgoing longwave radiation (OLR) data may be used to evaluate to what degree the model analysis results are representative of the real atmosphere.

However, this will likely be a rather difficult task because the eastern Pacific is usually not an active convective area.

REFERENCES

Burpee, R. W., 1972: The origin and structure of easterly waves in the lower troposphere of North Africa. *J. Atmos. Sci.*, **29**, 77-90.

Burpee, R. W., 1974: Characteristics of North African easterly waves during the summers of 1968 and 1969. *J. Atmos. Sci.*, **31**, 1556-1570.

Chang, C.-P., V. F. Morris and J. M. Wallace, 1970: A statistical study of easterly waves in the western pacific: July-December 1964. *J. Atmos. Sci.*, **27**, 195-201.

Holton, J. R., 1971: A diagnostic model for equatorial wave disturbances: The role of vertical shear of the mean zonal wind. *J. Atmos. Sci.*, **28**, 55-64.

Hogan, T. F., and T. E. Rosmond, 1991: The description of the navy operational global atmospheric prediction system's spectral forecast model. *Mon. Wea. Rev.*, **119**, 1786-1815.

Krishnamurti, T. N. and N. Surgi, 1987: Observational aspects of summer monsoon. *Monsoon Meteorology*, C.-P. Chang and T. Krishnamurti, eds., Oxford University Press, 3-25.

Lau, A. K., and N. C. Lau, 1989: Observed structure and propagation characteristics of summertime synoptic-scale disturbances over the tropical western pacific. *East Asia and Western Pacific Meteorology and Climate*. P. Sham and C. -P. Chang, eds., World Scientist Publication C., 48-57.

Lau, K. H., and N. G. Lau, 1990: Observed structure and propagation characteristics of tropical summertime synoptic scale disturbances. *Mon. Wea. Rev.*, **118**, 1888-1913.

Liebmann, B., and H. H. Hendon, 1990: Synoptic-scale disturbances near the equator. *J. Atmos. Sci.*, **47**, 1463-1479.

Lindzen, R. S., 1967: Planetary waves on beta planes. *Mon. Wea. Rev.*, **95**, 441-451.

Madden, R. and J. Stokes, 1975: Evidence of global scale 5-day waves in a 73-year pressure record. *J. Atmos. Sci.*, **32**, 831-836.

Maruyama, T., 1968: Time sequences of power spectra of disturbances in the equatorial lower stratosphere in relation to the quasi-biennial oscillation. *J. Meteor. Soc. Japan*, **46**, 327-342.

Maruyama, T., 1968: Upward transport of westerly momentum due to large-scale disturbances in the equatorial lower stratosphere. *J. Meteor. Soc. Japan*, **47**, 245-254.

Matsuno, T., 1966: Quasi-geostrophic motions in the equatorial area. *J. Meteor. Soc. Japan*, **44**, 245-254.

Reed, R. J., 1962: On the cause of the 26-month periodicity in the equatorial stratospheric winds. *Meteor. Abhandlungen, Freien Universität Berlin*, **36**, 245-257.

Reed, R. J., D. C. Norquist and E. E. Recker, 1977: The structure and properties of African wave disturbances as observed during Phase III of GATE. *Mon. Wea. Rev.*, **105**, 317-333.

Riehl, H. 1948: On the formation of typhoons. *J. Meteor.*, **5**, 247-264.

Rosenthal, S. L., 1965: Some preliminary theoretical considerations of tropospheric wave motions in equatorial latitudes. *Mon. Wea. Rev.*, **93**, 605-612.

Tucker, G. B., 1964: Zonal winds over the equator. *Quart. J. Roy. Meteor. Soc.*, **90**, 405-423.

Wallace, J. M., and C. P. Chang, 1969: Spectrum analysis of large-scale wave disturbances in the tropical lower troposphere. *J. Atmos. Sci.*, **26**, 1010-1025.

Yanai, M., and T. Maruyama, 1966: Stratospheric wave disturbances propagating over the equatorial pacific. *J. Meteor. Soc. Japan*, **44**, 291-294.

Yanai, M., T. Maruyama, T. Nitta and Y. Hayashi, 1968: Power spectra of large-scale disturbances over the tropical pacific. *J. Meteor. Soc. Japan*, **46**, 308-323.

Yanai, M., and Y. Hayashi, 1969: Large-scale equatorial waves penetrating from the upper troposphere into the lower stratosphere. *J. Meteor. Soc. Japan*, **47**, 167-182.

Yanai, M., and M. Murakami, 1970: A further study of tropical wave disturbances by the use of spectrum analysis. *J. Meteor. Soc. Japan*, **48**, 185-197.

INITIAL DISTRIBUTION LIST

1.	Defense Technical Information Center Cameron Station Alexandria, VA 22304-6145	2
2.	Library, Code 52 Naval Postgraduate School Monterey, CA 93943-5002	2
3.	Chairman (Code OC/Co) Department of Oceanography Naval Postgraduate School Monterey, CA 93943-5000	1
4.	Chairman (Code MR/Hy) Department of Meteorology Naval Postgraduate School Monterey, CA 93943-5000	1
5.	Prof. Chih-Pei Chang (Code MR/Cp) Department of Meteorology Naval Postgraduate School Monterey, CA 93943-5000	2
6.	Prof. Tom Murphree Department of Meteorology Naval Postgraduate School Monterey, CA 93943-5000	1
7.	Prof. Pat Harr Department of Meteorology Naval Postgraduate School Monterey, CA 93943-5000	1
8.	Prof. J. M. Chen Department of Meteorology Naval Postgraduate School Monterey, CA 93943-5000	1
9.	LCDR William C. Swett PSC 473, Box 68 FPO AP 96349-2902	1
10.	Commanding Officer Fleet Numerical Oceanography Center Monterey, CA 93943-5005	1

11. Commanding Officer
Naval Oceanographic and Atmospheric
Research Laboratory
Stennis Space Center
MS 39529-5004 | 1

12. Superintendent
Naval Research Laboratory
NPS Annex, Code 7500
Monterey, CA 93943-5006 | 1